Petersen

CARLETON UNIVERSITY
SYSTEMS ENGINEERING

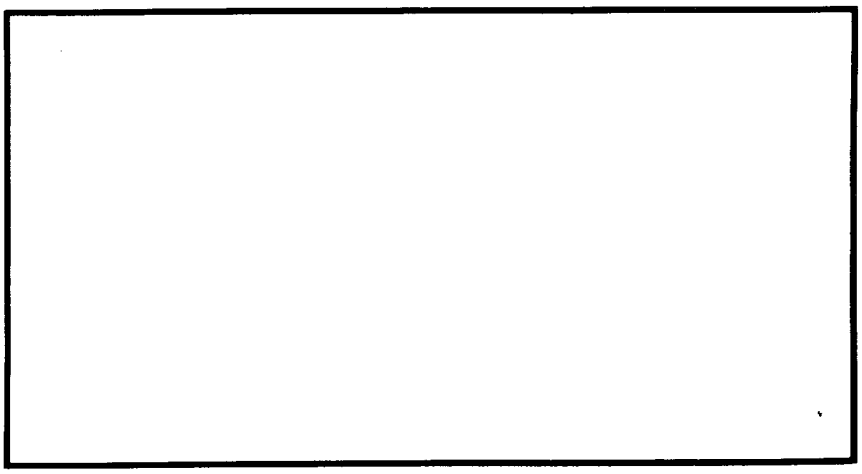

Department of Systems and Computer Engineering
Carleton University • Ottawa • Canada • K1S 5B6

Equalization in Cyclostationary Interference

Brent R. Petersen and David D. Falconer

Department of Systems & Computer Engineering
Carleton University
Ottawa, Canada K1S 5B6

January 1990

SCE-90-01

Petersen

Equalization in Cyclostationary Interference

by

Brent R. Petersen
David D. Falconer

Ottawa-Carleton Institute for Electrical Engineering
Faculty of Engineering
Department of Systems and Computer Engineering
Carleton University

January 8, 1990

Abstract

Communication channels where bandwidth efficiency is a prime concern suffer from interference (crosstalk), the principal performance-limiting impairment in many communications systems. Interference arises where communications systems lie in close proximity and it has two forms: co-channel interference and adjacent-channel interference. In twisted-pair subscriber loops, interference is in the form of co-channel interference. In radio channels, as in satellite, microwave, indoor wireless and digital cellular systems, it is in the form of co-channel and adjacent-channel interference. In these systems where the communication is digital, the baud rate clocks are similar, the systems use similar modulation techniques such as PAM, QAM or PSK, and there are only a few dominant or phase-aligned interferers, then the power of the interference can vary with period equal to the baud period, hence the term cyclostationary interference.

In this report, the linear equalizer receiver is analysed under the criterion of minimizing the mean square error in the presence multiple cyclostationary interferers and additive white noise. Furthermore this situation is compared to the case where the mean power spectrum of the interference is the same, but stationary. In order to provide more understanding of the analysis, a pedagogical example is presented. Some preliminary analysis for the zero-forcing and decision-feedback equalizer is also presented. Finally in the context of a subscriber loop system application the performance of the linear equalizer in the presence of cyclostationary interference and stationary noise is compared.

Acknowledgements

For their many helpful suggestions and comments, we thank the graduate students and staff of the Department of Systems and Computer Engineering, especially Majeed Abdulrahman, Prof. H. Hafez and Prof. M. El-Tanany.

We also thank TRIO, the Telecommunications Research Institute of Ontario, and the Cable Telecommunications Research Fellowship for their help in funding this research.

Table of Contents

List of Figures

Chapter 1

Introduction

1.1 Background

Communication channels where bandwidth efficiency is a prime concern suffer from interference, the principal performance-limiting impairment in many communications systems. Interference arises where communications systems lie in close proximity and it has two forms: co-channel interference and adjacent-channel interference. Adjacent-channel interference occurs when frequency-division multiplexed channels spill over into adjacent bands in the spectrum. Co-channel interference occurs when different systems use the same band but are only separated by some distance sufficient to ensure reasonable isolation.

With twisted-pair subscriber loops, interference is in the form of co-channel interference resulting from coupling among the various twisted pairs in a multipair cable. Increasing levels of interference occur with increasing baud rates since the crosstalk coupling loss increases with frequency [1, 2, 3]. Specifically, the dominant form of interference has an average power at the input to the receiver proportional to $|f|^{\frac{3}{2}}$. Interference in twisted-pair subscriber loops will be explored further in chapter 4.

With radio channels, as in satellite, microwave, indoor wireless and digital cellular systems, interference results from co-channel and adjacent-channel interference. In radio systems, increased levels of interference occur with closer physical spacing (higher co-channel interference) and narrower frequency allocation (higher adjacent-channel interference).

One difference between twisted-pair subscriber loops and radio channels which deserves a comment at this point is the mobility of the transmitters and receivers and the economics of choosing alternative channels. Twisted-pair subscriber loops have alternatives such as coaxial cable and optical fibres, but radio channels have no reasonable

alternative, assuming transmitter and/or receiver mobility is required[1]. However, the alternatives to subscriber loops, specifically optical fibre, are not economical for bit rates less than about $1\frac{M\ bits}{s}$, and that is for new installations [4]. One reason for the economics of choosing subscriber loops was the huge investment over the last 80 to 100 years by the telephone companies. At the time the loops were intended primarily for voice-band communication. However they have been shown to be suitable for basic rate ISDN (full duplex $144\frac{k\ bits}{s}$), noting the recent standard [5]. There are also standards for local area networks using twisted-pairs at $10\frac{M\ bits}{s}$ over short distances [6]. Finally, research in under way to put ISDN primary rate data on subscriber loops and it is in this application where interference is a major performance-limiting impairment [7, 8, 9, 10].

In the design of systems where interference is present, a question which needs to be considered is how much interference can be tolerated. This question is considered for subscriber loop systems and will be considered for digital cellular systems where the following four assumptions are valid: the communication is *digital* among the disturbed and disturbing systems, the symbol-rate clocks are *synchronized*[2] in frequency, the set of channels lying in close proximity are *modulated similarly* (e.g. baseband PAM, QAM, PSK, etc.) and there are a *few dominant*[3] or *phase-aligned*[4] interferers.

Under these four assumptions, the resulting interference becomes cyclostationary. That is, in such an environment the statistics (such as power) of the interference at the input to a receiver vary periodically in time, with a period equal to the baud period.

---

1 Just to make the terminology more confusing, the term subscriber loops is sometimes chosen to include end-point terminations using radio links, a proposal in future ISDN networks. However, for the remainder of this document the term subscriber loop will simply mean twisted-pair subscriber loop.

2 In subscriber loops the clock frequencies are synchronized since they are derived from a master clock [11]. However in radio systems the frequencies may be very similar, not strictly synchronized.

3 In subscriber loops, it is well known that there are usually only a few dominant interferers [12, 13]. The dominance of a few interferers in the radio channel is also being investigated [14].

4 Phase aligning interferers has been discussed in [1, 15].

This differs significantly from the case where the interference is only stationary noise and these differences will affect the design of the receiver.

An example of how the cyclostationarity of the interference affects the design of receivers will be demonstrated by the following brief example.

Figure 1.1 shows two possible transmitted signals and interference which is either stationary noise or cyclostationary interference. The noise and interference may be interpreted as part of the ensembles of their respective random processes. The problem for the receiver is to estimate which signal, either $+1$ or -1 was transmitted in the presence of the additive interference given that the receiver has knowledge about the statistics of the interference. Suppose further that the power spectrum of the stationary noise and cyclostationary interference are the same.

In the first case where the signal is corrupted stationary noise, the receiver would *equally* emphasize the signal components in region 1 and region 2 of Figure 1.1. However, in the second case where the signal is corrupted cyclostationary interference, the receiver would put more emphasis on the signal component in region 2 because the power of the interference is lower in region 2. Hence, the receiver will change depending on whether the interference is stationary or cyclostationary even if the interference has the same power spectrum.

The goal of this work is to show that the cyclostationary nature of interference can be exploited in equalization. Another goal is the comparison of the performances of equivalent systems with stationary and cyclostationary interference — This comparison will allow further evaluation of various clock synchronization strategies in interference-limited systems.

1.2 Completed Analysis

Chapters 2, 3 and 4 describe the completed analysis.

Chapter 2 describes the model of the cyclostationary interference used in later chapters. This chapter also introduces some of the effects on interference when it is bandlimited.

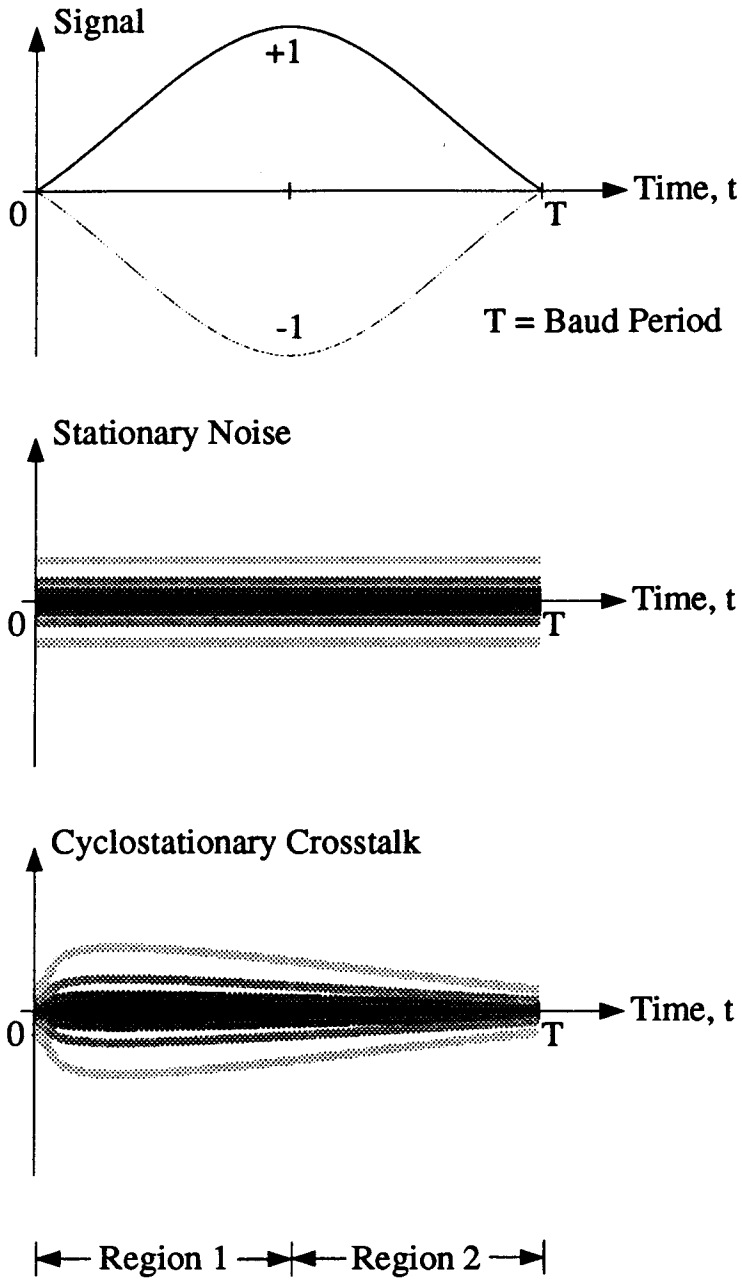

Figure 1.1 Stationary versus Cyclostationary Interference

Chapter 3 contains more rigorous developments on the effect of cyclostationary interference on receivers. Linear and decision-feedback equalizers are analysed where the performance criterion is the mean square error (MSE) and the interference at the input to the receivers is additive cyclostationary interference plus white noise. Also, the zero-forcing equalizer is considered since it provides additional insight. Note that to assess the performance limits of equalization in cyclostationary interference, continuous-time equalizers with no constraint on complexity are considered. Furthermore, these receivers are also compared to the case where in the interference in the channel has the same power spectrum, but is stationary. To help clarify some of the differences between equalization in cyclostationary interference and stationary noise a pedagogical example is presented.

Chapter 4 describes an application with a linear equalizer working in the presence of cyclostationary subscriber loop interference. It is compared to the case where the same type of equalizer is operating in stationary noise with the same power spectrum as in the cyclostationary case. This comparison will illustrate that the cyclostationary property is exploited by the equalizer to yield better performance than for the stationary noise case.

Chapter 2

Cyclostationary Interference

2.1 System and Interference Model

The interference and system model are shown in Figure 2.1. In this model $\phi_0(t)$ is the convolution of both the pulse and the channel impulse responses. The signal component at the input to the receiver is given by

$$s(t) = \sum_{n=-\infty}^{\infty} d_{n_0}\, \phi_0(t - nT) \tag{2.1}$$

where d_{n_0} are the transmitted data and T is the baud period. The i^{th} interferer, $\phi_i(t)$, is the convolution of both the pulse and the i^{th} interferer's impulse response. Thus the total interference at the input to the receiver due to all interferers and noise is given by

$$\nu(t) = n(t) + \sum_{i=1}^{\infty} \sum_{n=-\infty}^{\infty} d_{n_i}\, \phi_i(t - nT) \tag{2.2}$$

where $n(t)$ is noise and d_{n_i} are the data of the i^{th} interferer. The baseband noise has a two-sided power spectrum N_0 and is white:

$$\begin{aligned} E[n(t)] &= 0 \\ E[n(t_1)\, n^*(t_2)] &= N_0\, \delta(t_1 - t_2) \end{aligned} \tag{2.3}$$

$\delta(t)$ is the unit impulse ($*$ denotes complex conjugate). The data among the signal and all interferers are statistically independent with mean zero and variance one. The variance of the data, σ_d^2, can be assumed to be one without loss of generality because it is equivalent to putting the scaling factor into the pulse shape instead of the data.

$$\begin{aligned} E[d_{n_i}] &= 0 \\ E[d_{n_i} d^*_{m_k}] &= \sigma_d^2\, \delta_{i-k}\, \delta_{n-m} \\ \sigma_d^2 &= 1 \\ \delta_k &= \begin{cases} 1 & , k = 0 \\ 0 & , k \neq 0 \end{cases} \end{aligned} \tag{2.4}$$

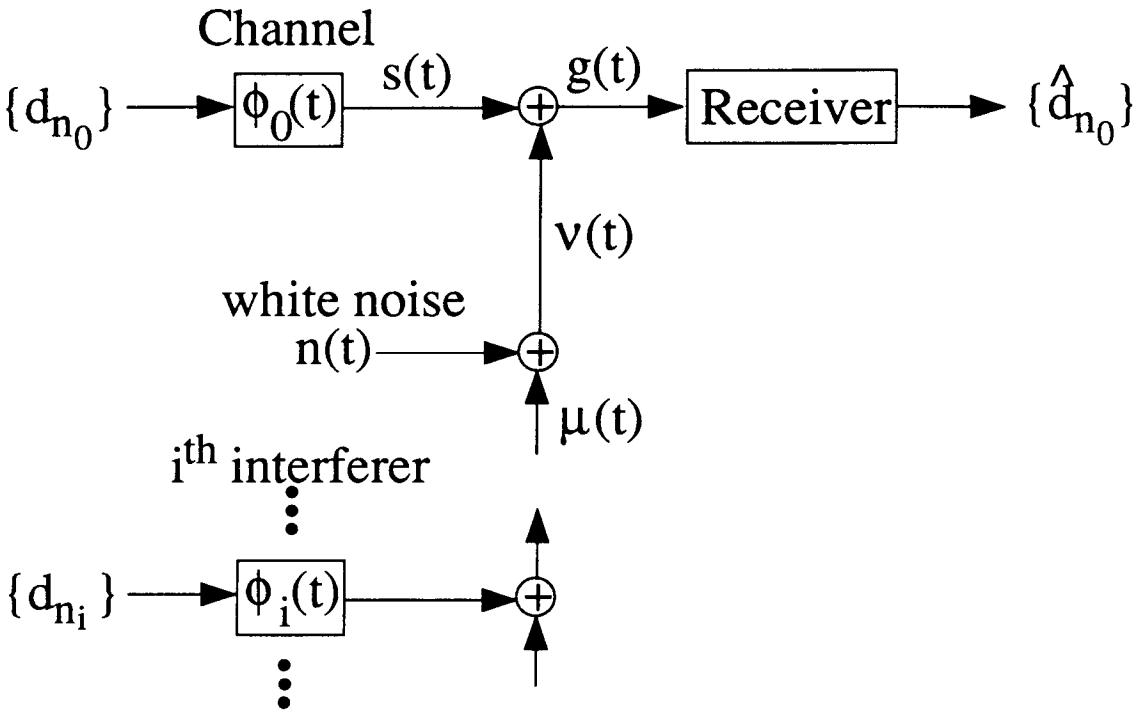

Figure 2.1 System and Interference Model

The input to the receiver is the sum of the signal and interference components $g(t) = s(t) + \nu(t)$. This model is similar to the one described in [1].

Some of the inherent assumptions of this model will be described. The communication is digital where the channel and the interferers use the same synchronized baud-rate clocks. The channel and the interferers use the same modulation scheme (PAM, QAM, PSK, etc.). Since this model includes the complex baseband representation [16], the interference can include both co-channel and adjacent-channel interference. In the frequency domain the co-channel interference is centered at 0 Hz and the adjacent-channel interference would be centered at some non-zero frequency so that it would only be a vestigial component in the baseband frequencies.

One more inherent assumption of this system and interference model lies in the way in which the receiver is only able to observe one channel output. Generalizing, one could obtain a multiple input and output channel with a multi-channel receiver. Such a multiple input receiver could be thought of as a diversity combiner. However it may not always be practical to have a receiver with multiple inputs from multiple channel outputs. This is why the receivers will only be allowed to observe one channel output. This will be discussed further in chapter 3.

Due to the interferers, $\{\phi_i(t),\ i \geq 1\}$, the input to the receiver is in general cyclostationary. For the remainder of this chapter the white noise component will not be considered since it is stationary. Consider one interferer. Call the interference at the input to the receiver:

$$\nu_2(t) = \sum_{n=-\infty}^{\infty} d_{n_1}\ \phi_1(t - nT) \tag{2.5}$$

To observe the cyclostationarity of $\nu_2(t)$, the variance can be shown to be

$$E\left[|\nu_2(nT+\tau)|^2\right] = \sum_{m=-\infty}^{\infty} \left(\frac{1}{T} \int_{-\infty}^{\infty} \Phi_1\left(f + \frac{m}{T}\right)\ \Phi_1^*(f)\ df \right) e^{\frac{j2\pi\tau m}{T}} \tag{2.6}$$

which is an expression in the form of a Fourier series, where $\Phi_1(f)$ is the Fourier transform of $\phi_1(t)$ [17]. Equation (2.6) can be extended to give the variance of the sum

of all interferers at the input to the receiver:

$$E\left[|\mu(nT+\tau)|^2\right] = \sum_{m=-\infty}^{\infty}\left(\frac{1}{T}\int_{-\infty}^{\infty}\sum_{i=1}^{\infty}\Phi_i\left(f+\frac{m}{T}\right)\Phi_i^*(f)\,df\right)e^{\frac{j2\pi\tau m}{T}} \qquad (2.7)$$

$E\left[|\mu(nT+\tau)|^2\right]$ is periodic in τ with period T.

2.2 Bandwidth Effects

Equation (2.7) is a convenient form to consider the effect of bandwidth on cyclostationarity. The variance will be cyclostationary if there are non-zero terms in the summation over m, excluding m equal to zero. Stated another way, the variance would end up being stationary if the only non-zero term in the summation is the one for m equal to zero; this always occurs when the interferer, $\Phi_1(f)$, is strictly bandlimited to $\frac{1}{2T}$ [18]. Having $\{\Phi_i(f),\ i \geq 1\}$ of bandwidth greater than $\frac{1}{2T}$ is a necessary condition for cyclostationarity, but it is not sufficient since it may be still be possible to have zero-valued coefficients in the Fourier series of (2.7) for m not zero. For example, a rectangular received interference pulse over one baud period has an infinite bandwidth, but would cause stationary interference.[5]

The degree of cyclostationarity is the difference, usually measured in dB, between the peak and valley of the variance over one baud period. If the interferers are bandlimited to $\frac{1}{T}$, then from equation (2.7) the variance of the interference can be written as:

$$E\left[|\nu_3(nT+\tau)|^2\right] = K_1 + K_2\cos\left(\frac{2\pi\tau}{T} + K_3\right) \qquad (2.8)$$

and the degree of cyclostationarity would be:

$$D = 10\ log_{10}\left(\frac{K_1+K_2}{K_1-K_2}\right) \qquad (2.9)$$

---

[5] Example due to Prof. M. El-Tanany

The dependency of the degree of cyclostationarity on the baud rate will affect the practicality of exploiting the cyclostationary behaviour of the interference in equalization. The degree of cyclostationarity will be discussed further in chapter 4 in the context of the subscriber loop application.

Chapter 3

Receiver Theory

3.1 Problem Formulation

The receiver shown in Figure 2.1 will be analysed for the specific cases of a continuous-time linear equalizer, continuous-time zero-forcing equalizer, and decision-feedback equalizer with a continuous-time forward filter. Continuous-time equalizers, that is equalizers with no constraint on complexity, are used in order to derive performance bounds of synchronous or fractionally-spaced equalizer implementations.

The performance criterion that will be used to analyse the linear and decision-feedback equalizers is the mean square error (MSE). The MSE was chosen because of three reasons. First, it makes the analysis of the receivers tractable. Second, it provides an exponentially-tight upper bound on the probability of error [19]. Third, an efficient means of implementing equalizers is using adaptive filters and the performance criterion which they minimize is the MSE [20, 21, 22].

The system and interference model of chapter 2 will be used in the analysis of this chapter. At any point in the following developments, the interferers can be set to zero and the developments will immediately revert to the familiar situation of a channel with just additive white noise.

3.2 Linear Equalizer Analysis

3.2.1 Cyclostationary Interference

The linear equalizer receiver is shown in Figure 3.1.

Given the known channel, $\{\phi_0(t)\}$, and co-channels, $\{\phi_i(t),\ i \geq 1\}$, of chapter 2, the mean and variance of the data being zero and one, all the data and white noise statistically independent, and the two-sided power spectrum of the baseband white noise

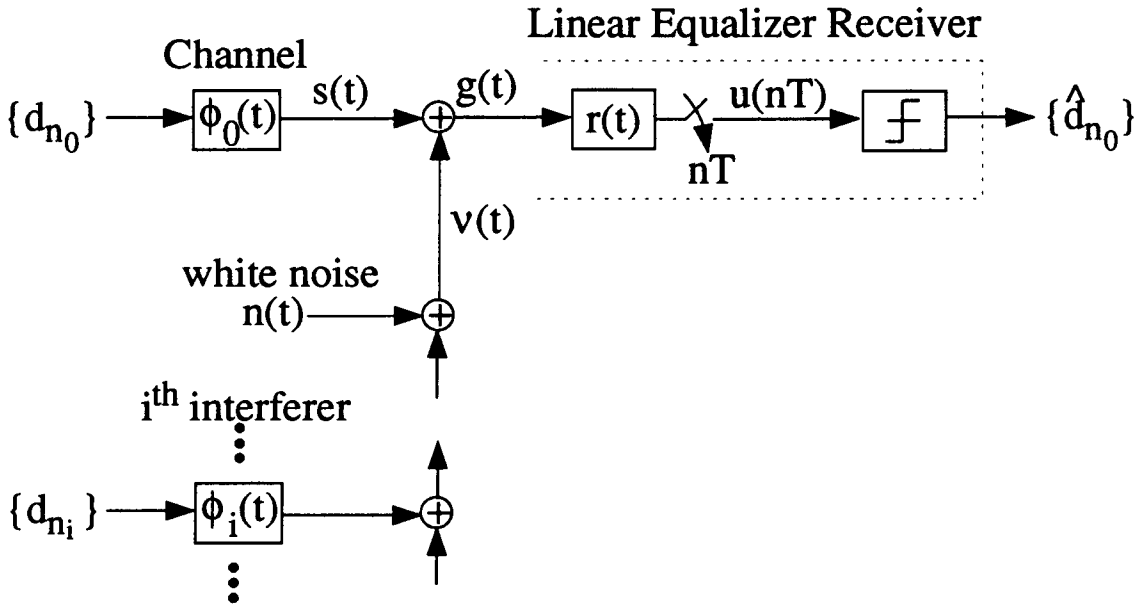

Figure 3.1 Linear Equalizer Receiver

being N_0, then the problem is to find $r(t)$ to minimize the MSE of the filter output sampled at the baud rate:

$$\varepsilon = E\left[\left|u(nT) - \widehat{d_{n_0}}\right|^2\right] \tag{3.1}$$

Correct decisions will be assumed ($\widehat{d_{n_0}} = d_{n_0}$). Thus the derivation is for a lower bound on the MSE and is a generalization of the additive white noise development [23].

Before proceeding further with the analysis, it will be put in perspective with some similar work described in the literature. Having set up the problem and notation, the discussion about this issue is easier.

In chapter 2, it was mentioned how a channel with interference may be viewed in a larger sense as a multiple-input multiple-output channel. In [24, 25], the authors analyse one multiple-input multiple-output channel with one multiple-input multiple-output co-channel and additive white noise. Their analysis proceeds using matrices and if the dimensions of those matrices are set to one, they derive the case of the optimal MSE linear equalizer with just one interferer and additive white noise. Since the authors consider multiple-input and multiple-output channels, their work has the following interpretation. Consider Figure 3.2. Two different systems are presented that have different tradeoffs between performance and complexity. For simplicity, they are only shown as a two-input two-output channel without interferers, but the discussion can easily be generalized to multiple-inputs and multiple-outputs with multiple interferers. The first system is more complex but can achieve a better MSE performance because it does an optimal diversity combining, similar to the work in [26]. It relies on access to all channel outputs. The higher complexity system based on a linear equalizer receiver has been previously analysed with a multiple-input multiple-output channel having additive white noise, but without explicit interferers [27, 28].

There is one more subtlety of the multiple-input multiple-output channel without explicit interferers to be noted. This case can include interferers by judiciously setting to zero some of the components of the cross-coupled channel before any receiver optimization. For example, in Figure 3.2a set $p_{10}(t)$, $p_{01}(t)$, $c_{01}(t)$ and $c_{11}(t)$ to

zero. Finding the optimal receiver matrix would result in the only non-zero elements being $r_{00}(t)$ and $r_{01}(t)$. The filter $r_{01}(t)$ could be discarded and this would leave $r_{00}(t)$ being the minimum MSE linear equalizer in cyclostationary interference and additive white noise. Thus the presence of interferers can be modelled as a specific case of the situation without interferers; it simply requires a sparse[6] cross-coupled channel matrix. Hence the most general analysis is in [27].

The lower-complexity system in Figure 3.2 is the one which will be analysed in this work. Note that the receivers in the lower complexity system, $\{r_0(t),\ r_1(t)\}$, will, in general, be different from those corresponding to the system with the higher performance $\{r_{00}(t),\ r_{11}(t)\}$.

The higher complexity systems are not treated here since in many practical situations, both or all of the channel outputs are not available at the same location[7] and even if they are available, the cost of the higher complexity system may not be warranted in view of the performance gained. There are situations where multiple channel outputs are available. In [24, 25] they refer to the situation where a twisted pair cable may have all its outputs terminated at a single physical location. In [28, 19], they describe cross-polarized radio channels with two channels whose outputs are fed into linear and decision-feedback equalizers of the higher complexity type (see Figure 3.2).

Note that in none of the previously mentioned works do the authors make a comparison between the receiver performances for stationary and cyclostationary interference of a given power spectrum.

The optimal MSE linear equalizer receiver to be developed here has already been determined by a different approach [29, 30]. The analysis of the familiar linear equalizer [31] is included here as a stepping stone to the more complex analysis of the decision-feedback equalizer shown later in this chapter. It is also included to provide a framework for comparing the linear equalizer performance in cyclostationary interference versus stationary noise.

---

6 A sparse matrix means many of the elements of the matrix are zero.

7 An exception occurs in radio systems with diversity.

[a] Higher Performance System :

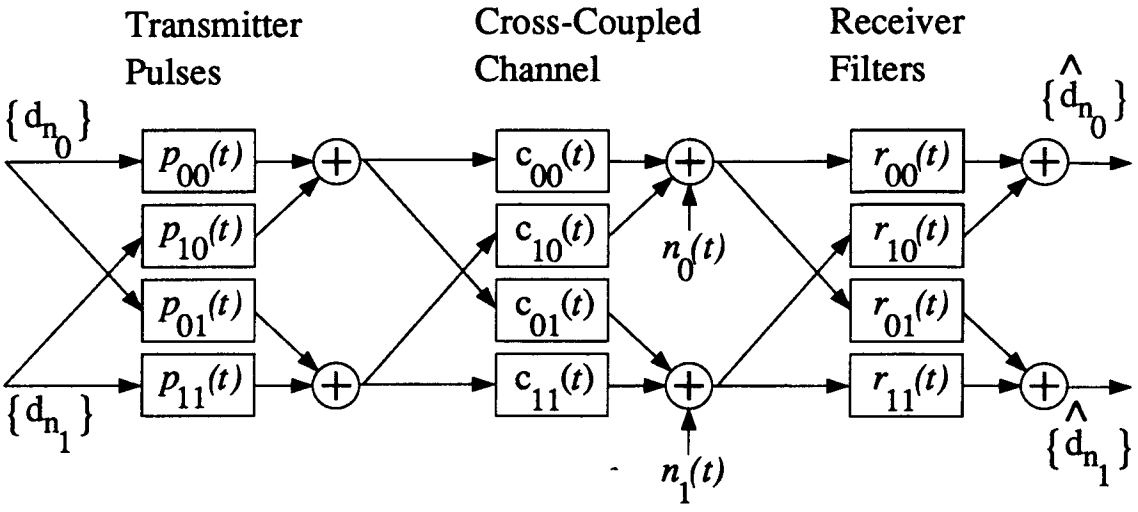

[b] Lower Complexity System :

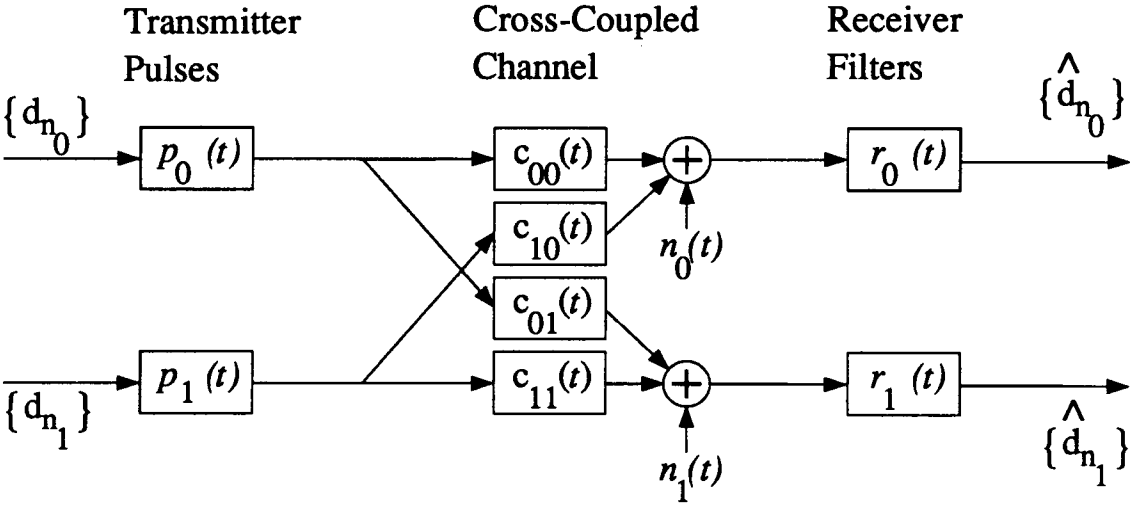

Figure 3.2 Multiple-Input Multiple-Output Channel

Proceeding with the analysis of the one-output system, from equation (3.1), the MSE may be rewritten as:

$$\varepsilon = E\left[u\left(nT\right)u^{*}\left(nT\right)\right] - E\left[d_{n_0}u^{*}\left(nT\right)\right] - E\left[d_{n_0}^{*}u\left(nT\right)\right] + E\left[d_{n_0}d_{n_0}^{*}\right] \tag{3.2}$$

But $u\left(nT\right)$ may be expressed as signal and interference components which have been filtered by the receiver:

$$\begin{aligned} u\left(nT\right) = & \sum_{m=-\infty}^{\infty} d_{m_0} \int_{-\infty}^{\infty} \phi_0\left(\tau\right)\, r\left(\left(n-m\right)T-\tau\right)\, d\tau \\ & + \int_{-\infty}^{\infty} \nu\left(\tau\right)\, r\left(nT-\tau\right)\, d\tau \end{aligned} \tag{3.3}$$

Substituting $u\left(nT\right)$ from (3.3) into (3.2) and evaluating the expectations over the data and white noise, the four terms of the MSE become:

$$\begin{aligned} \varepsilon = & \int_{-\infty}^{\infty}\int_{-\infty}^{\infty} k\left(t,\tau\right)\, r^{*}\left(t\right)\, r\left(\tau\right)\, d\tau\, dt + \int_{-\infty}^{\infty} \phi_0^{*}\left(-t\right)\, r^{*}\left(t\right)\, dt \\ & + \int_{-\infty}^{\infty} \phi_0\left(-t\right)\, r\left(t\right)\, dt + 1 \end{aligned} \tag{3.4}$$

$$k\left(t,\tau\right) = \sum_{i=0}^{\infty}\sum_{m=-\infty}^{\infty} \phi_i\left(mT-\tau\right)\, \phi_i^{*}\left(mT-t\right) + N_0\delta\left(t-\tau\right) \tag{3.5}$$

The problem is to find $r\left(t\right)$ which minimizes the MSE given in equation (3.4), and by the calculus of variations (see appendix A) the optimal function for $r\left(t\right)$, call it $r_o\left(t\right)$, satisfies the following integral equation:

$$\int_{-\infty}^{\infty} k\left(t,\tau\right)\, r_o\left(\tau\right)\, d\tau = \phi_0^{*}\left(-t\right) \tag{3.6}$$

Now the MSE, ε, can rewritten in terms of the optimal receiver filter:

$$\begin{aligned} \varepsilon_{\min} &= 1 - \int_{-\infty}^{\infty} \phi_0\left(-t\right)\, r_o\left(t\right)\, dt \\ &= 1 - \int_{-\infty}^{\infty} \Phi_0\left(f\right)\, R_o\left(f\right)\, df \end{aligned} \tag{3.7}$$

where $R_o\left(f\right)$ and $\Phi_0\left(f\right)$ are the Fourier transforms of $r_o\left(t\right)$ and $\phi_0\left(t\right)$, respectively.

Expanding the integral in equation (3.6) and grouping all integrals over $d\tau$ into constants which are not functions of t and rearranging gives the form of the optimal filter (provided $N_0 \neq 0$):

$$r_o(t) = \sum_{i=0}^{\infty} \sum_{n=-\infty}^{\infty} c_{n_i} \, \phi_i^*(nT - t) \tag{3.8}$$

For the moment the specific values of c_{n_i} are not important, however the form of equation (3.8) is. It indicates that the optimal linear equalizer can be interpreted as a bank of filters matched to the individual $\{\phi_i(t)\}$ as shown Figure 3.3. Note that for the case of just additive white noise in the channel (all interferers zero), Figure 3.3 reverts to the familiar form of a matched filter followed by a synchronous equalizer.

Equation (3.6) may be solved by taking Fourier transforms with respect to t to give:

$$N_0 \, R_o(f) + \frac{1}{T} \sum_{i=0}^{\infty} \Phi_i^*(f) \sum_{l=-\infty}^{\infty} \Phi_i\left(f + \frac{l}{T}\right) R_o\left(f + \frac{l}{T}\right) = \Phi_0^*(f) \tag{3.9}$$

where $\{\Phi_i(f)\}$ are the Fourier transforms of $\{\phi_i(t)\}$, respectively. Equation (3.9) gives the optimal receiver in terms of the channel, the interferers and the white noise.

For $\{\Phi_i(f),\ i \geq 0\}$ strictly bandlimited to $\frac{1}{2T}$, $R(f)$ can be determined by rearranging equation (3.9):

$$R_{c_1}(f) = \begin{cases} 0 & , |f| \geq \frac{1}{2T} \\ \dfrac{\Phi_0^*(f)}{N_0 + \frac{1}{T} \sum_{i=0}^{\infty} |\Phi_i(f)|^2} & , |f| < \frac{1}{2T} \end{cases} \tag{3.10}$$

This will be compared to a result for stationary noise in the next section.

For $\{\Phi_i(f),\ i \geq 0\}$ strictly bandlimited to $\frac{1}{T}$, $R(f)$ can be determined from a system of three equations and three unknowns obtained by replacing f in equation (3.9) by $f + \frac{1}{T}$, f and $f - \frac{1}{T}$. When this system is solved it gives the form of the optimal

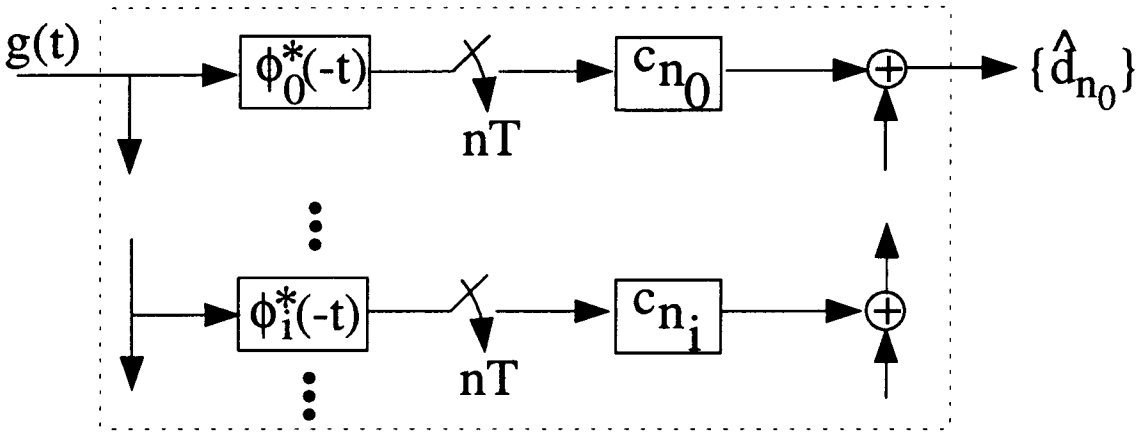

Figure 3.3 Form of the Minimum MSE Linear Equalizer

receiver:

$$R_{c_2}(f) = \begin{cases} 0 & , |f| \geq \frac{1}{T} \\ \dfrac{\begin{vmatrix} V_0(f-\frac{1}{T}) & \Phi_0^*(f-\frac{1}{T}) & 0 \\ V_1^*(f-\frac{1}{T}) & \Phi_0^*(f) & V_1(f) \\ 0 & \Phi_0^*(f+\frac{1}{T}) & V_0(f+\frac{1}{T}) \end{vmatrix}}{\begin{vmatrix} V_0(f-\frac{1}{T}) & V_1(f-\frac{1}{T}) & 0 \\ V_1^*(f-\frac{1}{T}) & V_0(f) & V_1(f) \\ 0 & V_1^*(f) & V_0(f+\frac{1}{T}) \end{vmatrix}} & , |f| < \frac{1}{T} \end{cases} \tag{3.11}$$

where

$$V_0(f) = N_0 + \frac{1}{T}\sum_{i=0}^{\infty} |\Phi_i(f)|^2 \tag{3.12}$$

and

$$V_1(f) = \frac{1}{T}\sum_{i=0}^{\infty} \Phi_i^*(f)\ \Phi_i\left(f+\frac{1}{T}\right) \tag{3.13}$$

Results of the same character, with larger-dimensional matrices, can be obtained for the cases where the bandwidth of $\{\Phi_i(f), i \geq 0\}$ exceeds $\frac{1}{T}$.

An important note about this receiver is that it is time-invariant. Even though at one point in the development the optimal receiver can be determined from a time-variant deconvolution (see equation 3.6). Since the MSE is minimized only at baud rate samples, and since the output of the channel is stationary when sampled at the baud rate, even though the continuous signals and interference in the channel are cyclostationary, the receiver is still time-invariant. If instead an MSE minimization was performed in continuous-time throughout the baud period, the receiver would in general be time-variant [18].

3.2.2 Stationary Interference

These results for the cyclostationary interference will now be compared to linear equalizer performance in stationary noise. Many of the equations to be shown are well known for stationary noise. The purpose of presenting them is to relate them to the similar results for the cyclostationary case.

In Figure 3.1 the mean power spectrum of the interference (averaged over one baud period) is:

$$\overline{S_{\nu\nu}}(f) = N_0 + \frac{1}{T}\sum_{i=1}^{\infty}|\Phi_i(f)|^2 \tag{3.14}$$

$\overline{S_{\nu\nu}}(f)$ was derived from the power spectrum of a QAM signal [16, 32]. If the interference shown in Figure 3.1 is replaced with stationary noise having the same power spectrum as equation (3.14), the minimum MSE linear equalizer can be determined by whitening [33] the noise in the channel and yields the following:

$$R_s(f) = \frac{\Phi_0^*(f)}{N_0 + \frac{1}{T}\sum_{i=1}^{\infty}|\Phi_i(f)|^2 + \frac{1}{T}\sum_{l=-\infty}^{\infty}\frac{N_0+\frac{1}{T}\sum_{i=1}^{\infty}|\Phi_i(f)|^2}{N_0+\frac{1}{T}\sum_{i=1}^{\infty}|\Phi_i(f+\frac{l}{T})|^2}\left|\Phi_0\left(f+\frac{l}{T}\right)\right|^2} \tag{3.15}$$

$R_s(f)$ is put in this form in order to compare it to the cyclostationary interference result in equation (3.11).

When the interferers $\{\Phi_i(f),\ i \geq 1\}$ in equation (3.15) are zero, $R_s(f)$ reverts to the following familiar form for a channel with just white noise [23, 34]:

$$R_{s_1}(f) = \frac{\Phi_0^*(f)}{N_0 + \frac{1}{T}\sum_{l=-\infty}^{\infty}\left|\Phi_0^*\left(f+\frac{l}{T}\right)\right|^2} \tag{3.16}$$

When the interferers $\{\Phi_i(f),\ i \geq 1\}$ in equation (3.15) are strictly bandlimited to $\frac{1}{2T}$, $R_s(f)$ takes on the following form:

$$R_{s_2}(f) = \begin{cases} 0 & ,|f| \geq \frac{1}{2T} \\ \frac{\Phi_0^*(f)}{N_0+\frac{1}{T}\sum_{i=0}^{\infty}|\Phi_i(f)|^2} & ,|f| < \frac{1}{2T} \end{cases} \tag{3.17}$$

Note that equation (3.17), is identical to the cyclostationary result in equation (3.10) and this was to be expected since the interference becomes stationary when strictly bandlimited to $\frac{1}{2T}$ (see equation (2.7)).

When the interferers $\{\Phi_i(f),\ i \geq 1\}$ in equation (3.15) are strictly bandlimited to $\frac{1}{T}$, $R_s(f)$ takes on a completely different form than the cyclostationary case given in equation (3.11). This means that the performance in stationary and cyclostationary interference is not the same and the performance improvements obtained in cyclostationary interference will be demonstrated in the subscriber loop system application in chapter 4.

3.2.3 Pedagogical Example

To gain further insight into the previous analysis and how equalization in cyclostationary interference differs from that of stationary noise, the following pedagogical example was constructed. The results shown here are for a system whose pulses and channels are not realistic. But more importantly the results show an exaggeration of the MSE tradeoffs that would occur in a realistic system.

Figure 3.4 contains a block diagram of the system. The transmitted data are d_{n_0}. The data of the single interferer are d_{n_1}. The pulse, channel and co-channel will be described below; the only reason for these particular choices is because they are sufficient for demonstration.

$raisedc\,(f)$ is the transmitted pulse described in the frequency domain where T is the baud period:

$$raisedc\,(f) = \begin{cases} 0 & ,|f| \geq \frac{1}{T} \\ \frac{1+\cos(\pi T f)}{2} & ,|f| < \frac{1}{T} \end{cases} \tag{3.18}$$

$cflat\,(f)$ is the channel frequency response:

$$\begin{aligned} cflat\,(f) &= 3.852 \times 10^{-3}\ rect\left(\frac{Tf}{2}\right) \\ rect\,(f) &= \begin{cases} 0 & ,|f| \geq \frac{1}{2} \\ 1 & ,|f| < \frac{1}{2} \end{cases} \end{aligned} \tag{3.19}$$

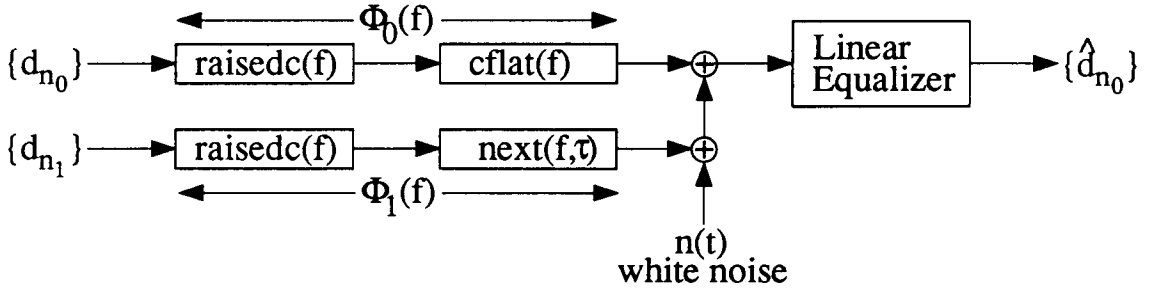

Figure 3.4 Pedagogical System

$next\ (f,\tau)$ is the coupling from the co-channel into the channel:

$$next\ (f,\tau)\ =\ \left(\frac{K_n}{2}\,|f|^{\frac{3}{2}}\right)^{\frac{1}{2}}\ e^{-j\,\frac{3\pi}{8}\,sgn(f)}\ \ delay\ (\tau,f)$$

$$K_n\ =\ 10^{-13}$$

$$sgn\ (f)\ =\ \begin{cases} -1 & ,f<0 \\ 0 & ,f=0 \\ +1 & ,f>0 \end{cases} \tag{3.20}$$

$$delay\ (\tau,f)\ =\ e^{-j2\pi f\tau}$$

τ is included as an extra argument in $next$ in order to vary the relative position, in time, of the interference with respect to the transmitted signal. Hence τ is an element of the interval $[0,T]$. The baud rate is $\frac{1}{T}\ =\ 80\,000\ Hz$. The white noise has a power spectrum: $N_0\ =\ 5\times10^{-7}$. Finally note that the overall channel is:

$$\phi_0\,(t)\ =\ raisedc\ (f)\ \ cflat\ (f) \tag{3.21}$$

and the overall co-channel is:

$$\phi_1\,(t)\ =\ raisedc\ (f)\ \ next\ (f,\tau) \tag{3.22}$$

The following definitions of $SINR$ (signal to interference-plus-noise ratio), SIR (signal to interference ratio) and SNR (signal to noise ratio) will be used:

$$SINR\ =\ 10\ log_{10}\left(\frac{P_S}{P_I\ +\ P_N}\right) \tag{3.23}$$

$$SIR\ =\ 10\ log_{10}\left(\frac{P_S}{P_I}\right) \tag{3.24}$$

and

$$SNR\ =\ 10\ log_{10}\left(\frac{P_S}{P_N}\right) \tag{3.25}$$

Referring to Figure 2.1, the average signal power is:

$$P_S\ =\ \frac{1}{T}\int_0^T E\left[|s\,(t)|^2\right]\ dt \tag{3.26}$$

the bandlimited noise power is:

$$P_N = N_0 \left(2 \frac{1}{T}\right) \tag{3.27}$$

and the average interference power is:

$$P_I = \frac{1}{T} \int_0^T E\left[|\mu(t)|^2\right] dt \tag{3.28}$$

According to the definitions, the $SINR$ in this example was computed to be 20 dB.

The impulse response of $\phi_0(t)$ and the variance of the signal, $\sum_{n=-\infty}^{\infty} d_{n_0} \phi_0(t - nT)$, are plotted in Figures 3.5a and 3.5b, respectively. The impulse response of $\phi_1(t)$ and the combined variance of $\sum_{n=-\infty}^{\infty} d_{n_1} \phi_1(t - nT)$ plus the noise bandlimited to $|f| < \frac{1}{T}$ are plotted in Figures 3.6a and 3.6b, respectively. In the figures, the following variables and functions are equal: $N0\_ = N_0$, $f0\_ = \frac{1}{T}$, $T0\_ = T$, $Tau\_ = \tau$, $phi0\ (t) = \phi_0(t)$ and $phi1\ (t) = \phi_1(t)$.

Since $\phi_0(t)$ and $\phi_1(t)$ are bandlimited to $\frac{1}{T}$, the optimal receiver for cyclostationary interference can be obtained from equations (3.11), (3.12) and (3.13) and it is plotted in Figure 3.7a. Similarly, the optimal receiver for stationary noise, having the same mean power spectrum as the cyclostationary interference, can be calculated from equation (3.15) and is shown in Figure 3.7b.

The striking difference between the receivers for the cyclostationary and stationary cases was the motivation for gaining more of an understanding of what the cyclostationary equalizer was doing. The reason for choosing the interference phase shift of

$$\begin{aligned} \tau &= Tau\_ \\ &= \tfrac{5}{8}T \\ &= 7.813 \times 10^{-6} \ \ seconds \end{aligned} \tag{3.29}$$

was to show the most striking difference.

Using equation (3.7), the MSE was calculated for various values of τ and plotted in Figure 3.8. The MSE also exhibits interesting behaviour at $\tau = \frac{5}{8}T$. The MSE for the stationary noise case was calculated using the same equation for the MSE but with

[a]

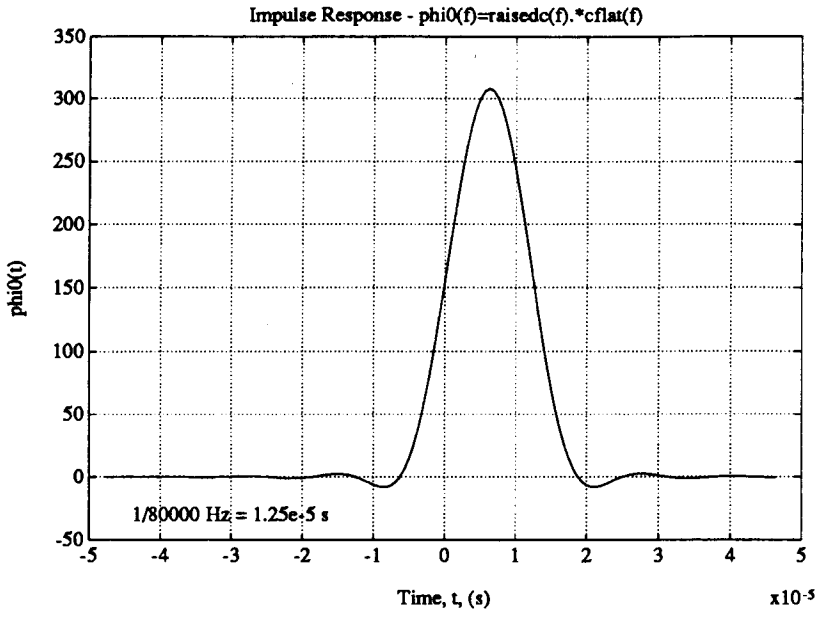

[b]

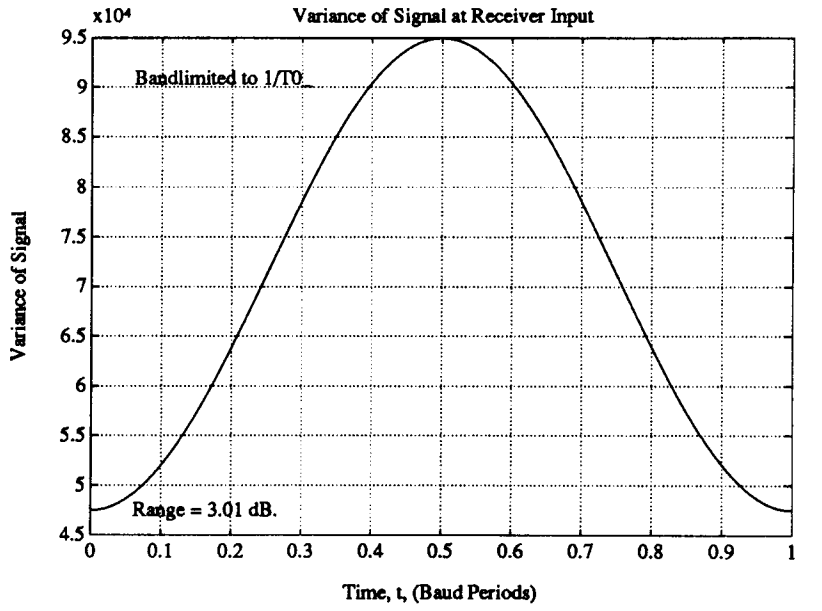

Figure 3.5 Impulse Response of Overall Channel and Variance of Signal

[a]

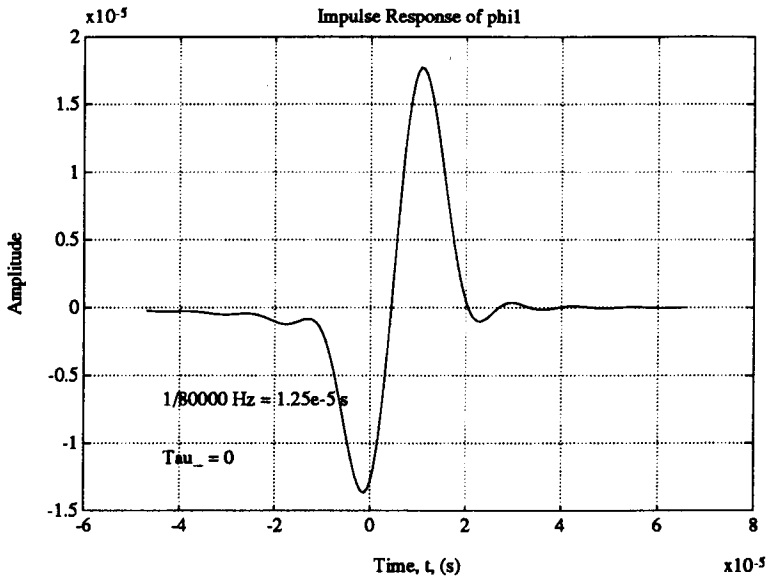

[b]

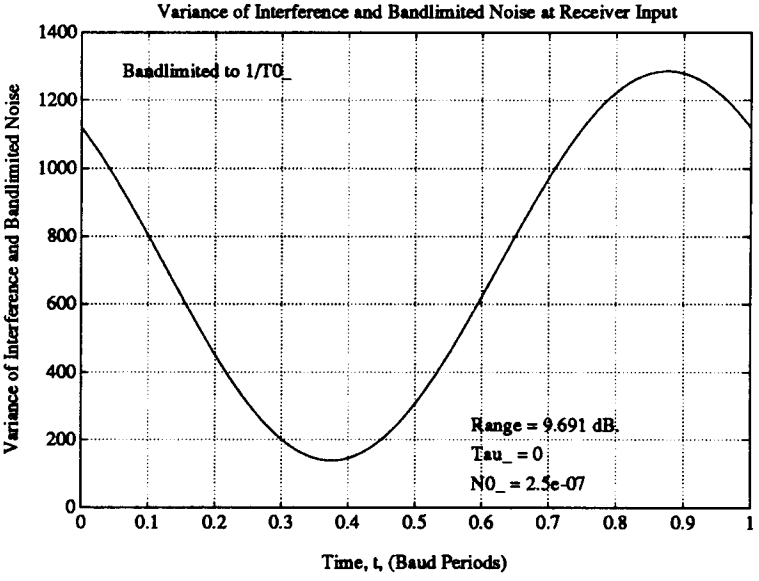

Figure 3.6 Impulse Response of Overall Co-Channel and Variance of Interference plus Noise

[a]

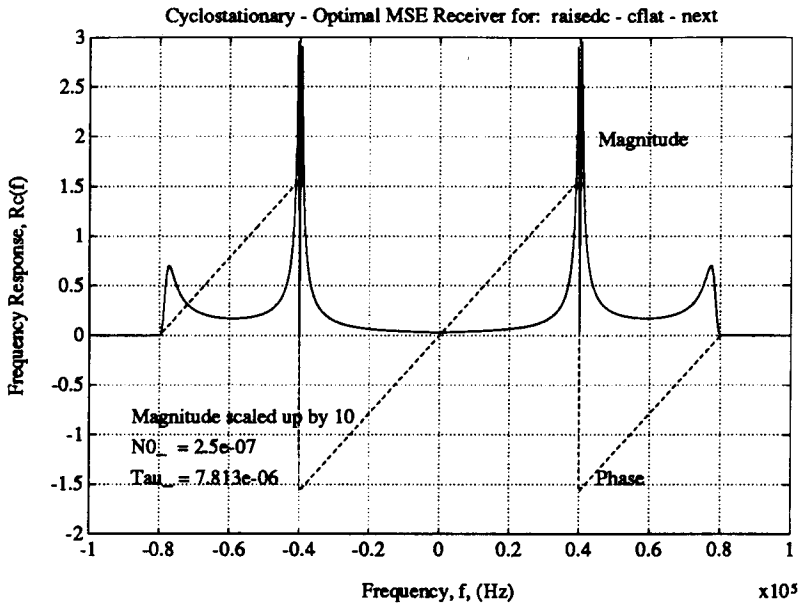

[b]

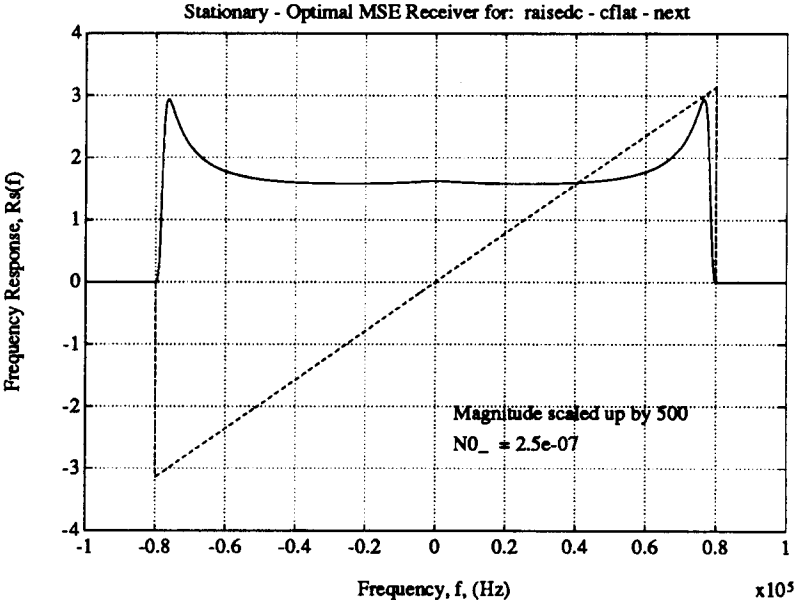

Figure 3.7 Optimal Cyclostationary and Stationary Receivers

the stationary noise receiver. The stationary noise MSE is shown in Figure 3.8 as a horizontal line.

The differences in the cyclostationary and stationary cases arise because in the cyclostationary case the MSE which must be minimized has an additional component due to the interference. Consider the MSE from equation (3.1) where $u(nT)$ from equation (3.3) can be expanded further to give:

$$\begin{aligned} u(nT) &= d_{n_0}\, h_0(0) + \sum_{m=-\infty\,,\, m\neq 0}^{\infty} d_{m_0}\, h_0((n-m)T) \\ &\quad + \sum_{m=-\infty}^{\infty} d_{m_1}\, h_1((n-m)T) \\ &\quad + \int_{-\infty}^{\infty} r(t)\; n(nT-t)\; dt \\ &\triangleq q_1 + q_2 + q_3 + q_4 \end{aligned} \tag{3.30}$$

where

$$h_i(t) = \phi_i(t) \star r(t)\;, \quad i \geq 0 \tag{3.31}$$

and $\star$ denotes convolution. Equation (3.30) can be substituted in equation (3.1) to give the following more meaningful interpretation of the MSE:

$$\varepsilon = \sigma^2_{data\ bias} + \sigma^2_{ISI} + \sigma^2_{Xtalk} + \sigma^2_{noise} \tag{3.32}$$

where

$$\begin{aligned} \sigma^2_{data\ bias} &= |h_0(0) - 1|^2 \\ \sigma^2_{ISI} &= E\left[|q_2|^2\right] \\ \sigma^2_{Xtalk} &= E\left[|q_3|^2\right] \\ \sigma^2_{noise} &= E\left[|q_4|^2\right] \end{aligned} \tag{3.33}$$

Recall that for a zero-forcing equalizer in stationary noise the terms $\sigma^2_{data\ bias}$ and σ^2_{ISI} are zero and the MSE is equal to just σ^2_{noise} but the MSE is higher than if all three terms are minimized. This situation occurs when Nyquist's First Criterion for zero intersymbol interference is satisfied; that is the sampled equalized channel, $h_0(nT)$, satisfies:

$$h_0(nT) = \begin{cases} 1 & , n = 0 \\ 0 & , n \neq 0 \end{cases} \tag{3.34}$$

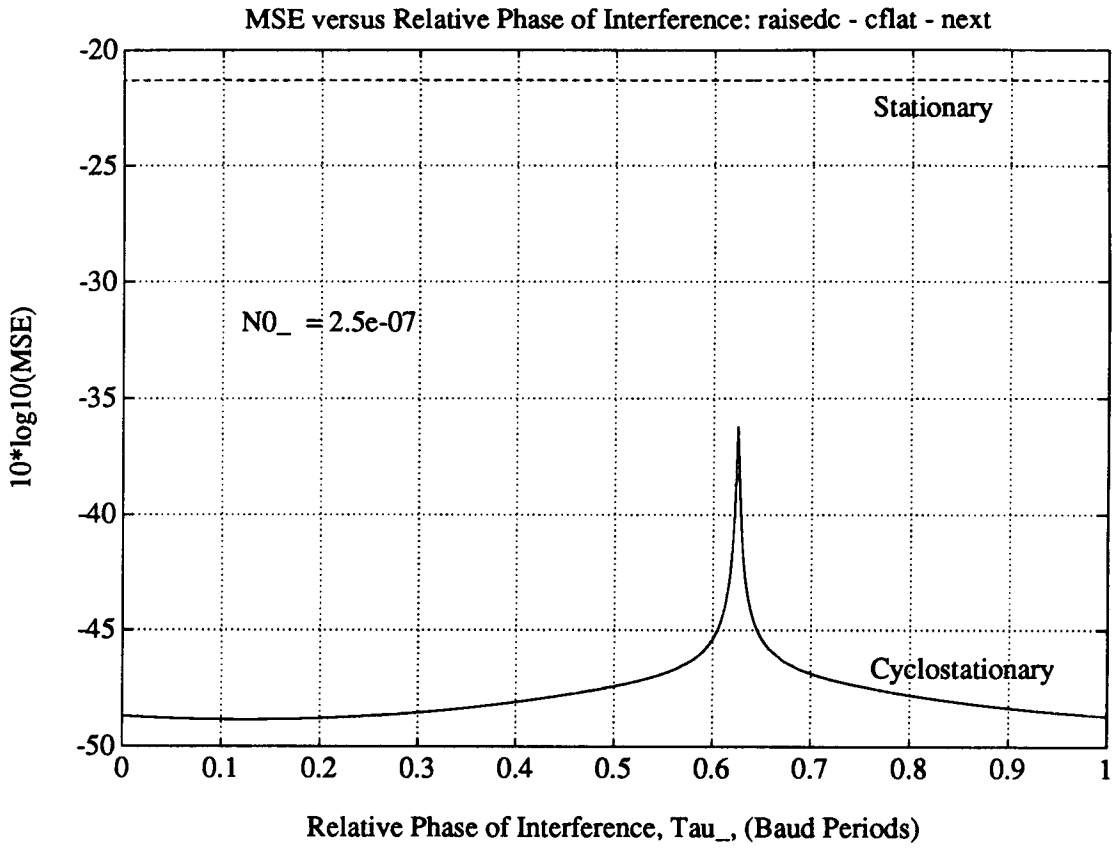

Figure 3.8 MSE versus Relative Interference Phase

However in the case of cyclostationary interference there is an extra term, σ^2_{Xtalk}. This term would be zero if it were possible to satisfy the following condition:

$$h_i(nT) = 0, \quad \forall n, \quad i \neq 0 \tag{3.35}$$

Nyquist might have called this his criterion for zero *co-channel* interference.

Note that as τ approaches $\frac{5}{8}T$, in Figure 3.5 the peak of the interference variance (see Figure 3.6b) is shifted to the right by $\frac{5}{8}T$ (or to the left by $\frac{3}{8}T$) and causes the position of the peak of the interference power to approach the position of the peak of the signal power (see Figure 3.5b). Thus $\tau = \frac{5}{8}T$ is the relative phase of the interference which results in the worst performance (see Figure 3.8). The receiver must suppress the interference component of the MSE more so at $\tau = \frac{5}{8}T$ than at any other phase. To do this, the previously mentioned condition for zero co-channel interference becomes more important. Since the receiver does not achieve this condition, but instead minimizes the total MSE, the receiver approaches the condition of zero co-channel interference more so at this phase than at any other.

Figures 3.9a and 3.9b contain the frequency responses of the sampled equalized channel and co-channel, respectively (i.e. the discrete-time periodic-frequency (DTPF) Fourier transforms of $h_0(nT)$ and $h_1(nT)$). The frequency response of the sampled equalized channel is what was expected from Nyquist's First Criterion; the magnitude is almost completely flat at a value of 1 for frequencies in the range $|f| \leq \frac{1}{2T}$. However, most of the energy of the sampled equalized co-channel is in two sharp peaks near $f = \pm\frac{1}{2T}$. In the time domain, the sampled equalized co-channel would be generally a sinusoidal of period roughly $\frac{1}{2T}$ having zero crossings at or near the sampling instants.

Figure 3.10 shows the impulse response of the equalized channel $h_0(t)$. The impulse response is of such long duration that its envelope is plotted in Figure 3.10a and it values in the neighbourhood of $t = 0$ are plotted in Figure 3.10b. Note that at $t = 0$ the value is at or near one and that at all the other sampling instants, the value is at or near zero. Figure 3.11 show the corresponding impulse response of equalized co-channel $h_1(t)$. Note that at all sampling instants the value is at or near zero.

[a]

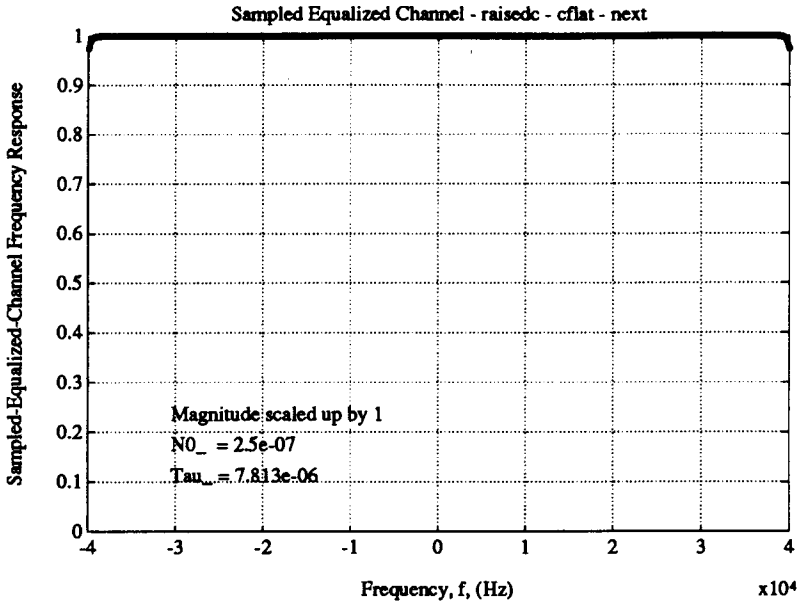

[b]

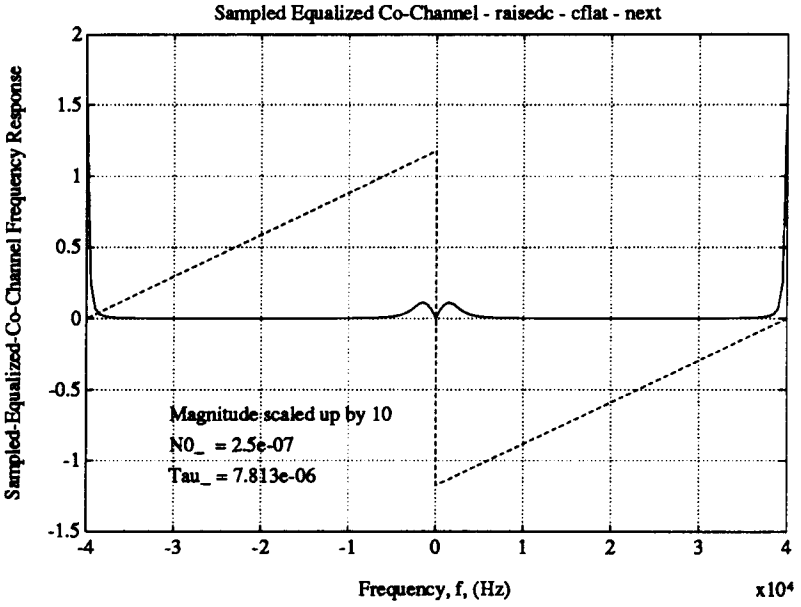

Figure 3.9 Sampled Equalized Channel and Co-Channel

[a]

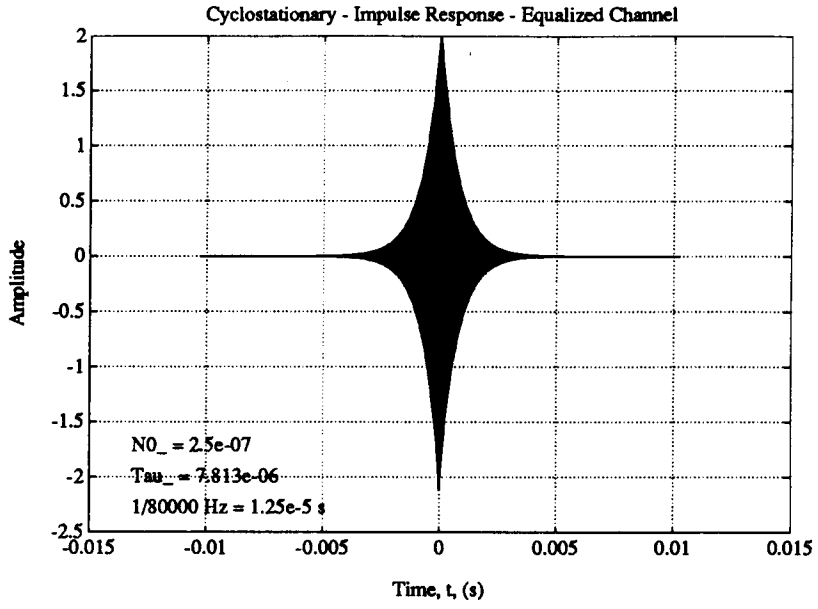

[b]

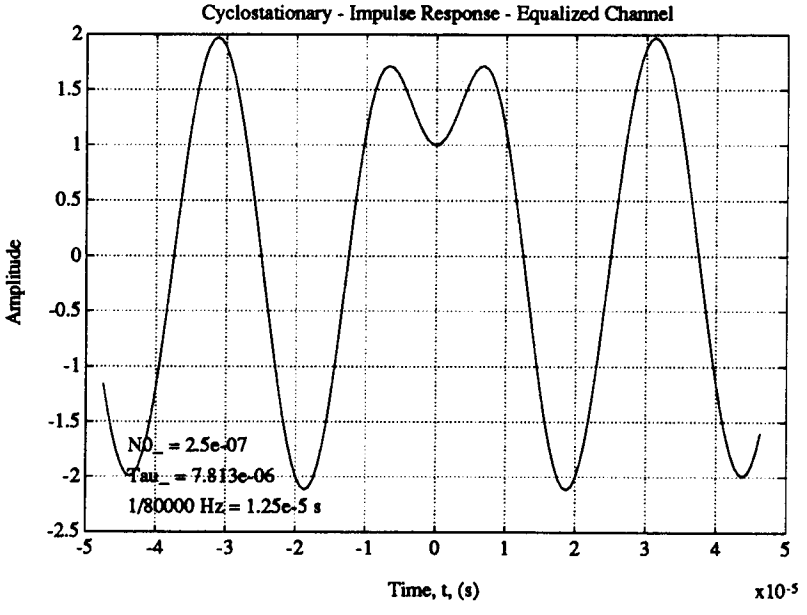

Figure 3.10 Impulse Response of Equalized Channel

[a]

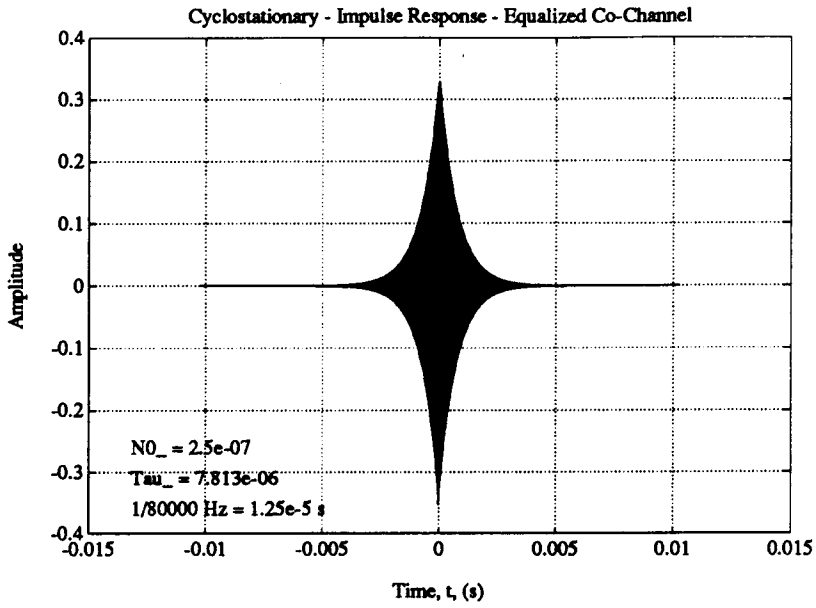

[b]

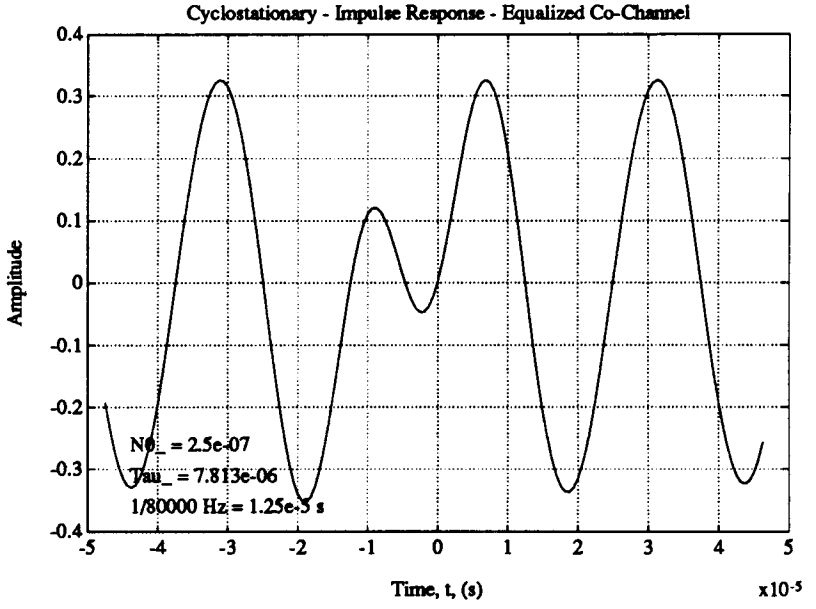

Figure 3.11 Impulse Response of Equalized Co-Channel

3.3 Zero-Forcing Equalizer Analysis

This section will briefly describe the zero-forcing equalizer and under what conditions it exists. It will give insight into both the linear and decision-feedback equalizers. The zero-forcing equalizer could be derived by letting N_0 approach zero in the linear equalizer analysis but the analysis to follow gives more insight.

Consider Figure 3.1 but where the additive white noise component, $n(t)$, is zero. Also let the equalized channels and co-channels be:

$$\begin{aligned} h_i(t) &= \phi_i(t) \star r(t) \\ H_i(f) &= \Phi_i(f)\ R(f) \end{aligned} \tag{3.36}$$

The condition for zero intersymbol interference is:

$$\frac{1}{T}\sum_{l=-\infty}^{\infty} H_0\left(f+\frac{l}{T}\right) = 1 \tag{3.37}$$

The condition for zero co-channel interference is:

$$\frac{1}{T}\sum_{l=-\infty}^{\infty} H_i\left(f+\frac{l}{T}\right) = 0 \quad ,i \geq 1 \tag{3.38}$$

These two conditions may be combined into the following:

$$\begin{aligned} \frac{1}{T}\sum_{l=-\infty}^{\infty} H_i\left(f+\frac{l}{T}\right) &= c_i \quad ,\forall i \\ c_i &= \begin{cases} 1 & ,i=0 \\ 0 & ,i\neq 0 \end{cases} \end{aligned} \tag{3.39}$$

Let there be only M interferers and therefore there are $N = M + 1$ independent data streams. Therefore the combined condition for the zero-forcing equalizer can be written as:

$$\frac{1}{T}\sum_{l=-\infty}^{\infty} \Phi_i\left(f+\frac{l}{T}\right) R\left(f+\frac{l}{T}\right) = c_i \quad ,0 \leq i \leq N-1 \tag{3.40}$$

Equation 3.40 represents N equations. If the overall channel and co-channels, $\{\Phi_i(f),\ i \geq 0\}$ are strictly bandlimited to $\frac{K}{2T}$, then at a given frequency, f, there will be up to K unknowns. For the case of K being an odd number, the unknowns are:

$$\left\{R\left(f+\frac{K-1}{2T}\right), \ldots, R\left(f-\frac{K-1}{2T}\right)\right\} \tag{3.41}$$

For the case of K being an even number, the unknowns are:

$$\left\{R\left(f+\frac{K-2}{2T}\right),\ldots,R\left(f-\frac{K}{2T}\right)\right\} \tag{3.42}$$

Thus, equation 3.40 will generally have a solution[8], that is there will be zero intersymbol interference and zero co-channel interference, when the number of equations is less than or equal to the number of unknowns. That is, the number of independent data streams is less than or equal to the number of the bandwidth:

$$N \leq K \tag{3.43}$$

From equation 3.40, the matrix involving $\{\Phi_i(f),\ i \geq 0\}$ for K being an odd number is:

$$\frac{1}{T}\begin{bmatrix} \Phi_0\left(f+\frac{K-1}{2T}\right) & \cdots & \Phi_0\left(f-\frac{K-1}{2T}\right) \\ \vdots & \ddots & \vdots \\ \Phi_{N-1}\left(f+\frac{K-1}{2T}\right) & \cdots & \Phi_{N-1}\left(f-\frac{K-1}{2T}\right) \end{bmatrix} \tag{3.44}$$

When the channels and co-channels have a frequency response which approaches zero at the high end of the frequency band, then the matrix's right column approaches zero. Hence, the matrix approaches singularity. This would mean that a zero-forcing equalizer would cause significant noise enhancement. Thus the analysis is more useful as insight into the flexibility of linear and decision-feedback equalizers to suppress multiple interferers in the cases where the bandwidth is large enough.

Considering the noise enhancement problem, note that the linear equalizer shown in the pedagogical example to follow later does not cause the sampled equalized co-channel (see equation 3.38) to be zero since the MSE is minimized instead. The equalized co-channel in the pedagogical example shows narrowband tones near $\pm\frac{1}{2T}$ instead of being zero. These tones mean that the impulse response passes through or near zero instead of zero at the sampling instants.

[8] Provided that the matrix involving $\{\Phi_i(f),\ i \geq 0\}$ is not singular for reasons such as some set of interferers or channel being identical. This is equivalent to the condition that the interferers and channel be linearly independent [25].

3.4 Decision-Feedback Equalizer Analysis

3.4.1 Cyclostationary Interference

The performance of a decision-feedback equalizer (DFE) receiver in cyclostationary interference is analysed in this section. This development is a generalization of the equivalent development for a DFE receiver at the output of a channel with just additive white noise [35, 36]. What is to be derived is a performance bound. That is the performance with no constraint on the tap spacing and number of taps in the forward filter. The DFE receiver is shown in Figure 3.12.

Given the known channel and co-channels, $\{\phi_i(t),\ i \geq 0\}$ of chapter 2, the mean and variance of the data being zero and one, all the data and white noise statistically independent, and the power spectrum of the white noise being N_0, then the problem is to find $r(t)$ and the coefficients of the feedback filter $\{b_k,\ k \geq 1\}$ to minimize the MSE:

$$\varepsilon = E\left[\left|w(nT) - \widehat{d_{n_0}}\right|^2\right] \tag{3.45}$$

Correct decisions will be assumed ($\widehat{d_{n_0}} = d_{n_0}$). Thus the derivation is for a lower bound on the MSE.

There have been results published in the literature for DFE receivers for multiple-input multiple-output channels. In [19], the authors consider a 2-input 2-output channel with a DFE receiver which also estimates the interference and subtracts it from the signal. Similar to the linear equalizer, the DFE which is analysed in this chapter is the lower complexity, but lower performance, structure in which receivers observe only *one* channel output. The additional assumption is made in the development to follow that the interference power at the receiver input is relatively small compared with the signal power; thus it is not reasonable to make reliable decisions on the interference data in order to subtract it from the received signal. These are the reasons why the DFE structure shown in Figure 3.12 was chosen. Also, the continuous-time analysis to follow has been previously done in discrete time with a finite number of tap coefficients [15].

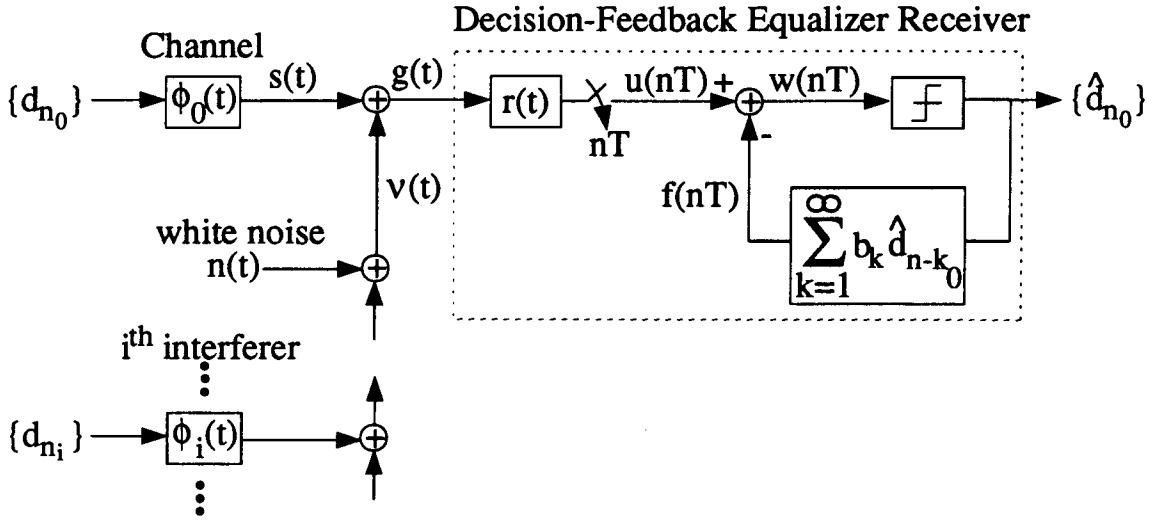

Figure 3.12 Decision-Feedback Equalizer Receiver

Proceeding with the analysis of the single-input receiver, from equation (3.45), the MSE may be rewritten as:

$$\varepsilon \;=\; E\left[w\left(nT\right)w^{*}\left(nT\right)\right] - E\left[d_{n_0}w^{*}\left(nT\right)\right] - E\left[d^{*}_{n_0}w\left(nT\right)\right] + E\left[d_{n_0}d^{*}_{n_0}\right] \tag{3.46}$$

But

$$w\left(nT\right) \;=\; u\left(nT\right) \;-\; f\left(nT\right) \tag{3.47}$$

where $u\left(nT\right)$ may be obtained from equation (3.3) and

$$f\left(nT\right) \;=\; \sum_{k=1}^{\infty} b_k \, d_{n-k_0} \tag{3.48}$$

In a stationary noise development of the DFE, to minimize the MSE requires the coefficients of the feedback filter, b_k, be set equal to the samples of the equalized channel. It can be shown that this is true for cyclostationary interference as well:

$$b_k \;=\; \int_{-\infty}^{\infty} \phi_0\left(kT-\tau\right)\; r\left(\tau\right)\; d\tau \tag{3.49}$$

This was to be expected since setting the coefficients this way makes the post-cursor ISI zero (assuming correct decisions). The coefficients can be set after $r\left(t\right)$ has been determined.

Substituting $w\left(nT\right)$, $f\left(nT\right)$ and b_k from (3.47), (3.48) and (3.49) into (3.46) and evaluating the expectations over the statistically independent data and white noise, the four terms of the MSE become:

$$\begin{aligned}\varepsilon \;=\; & \int_{-\infty}^{\infty}\int_{-\infty}^{\infty} k_2\left(t,\tau\right)\; r^{*}\left(t\right)\; r\left(\tau\right)\; d\tau\; dt \;+\; \int_{-\infty}^{\infty} \phi_0^{*}\left(-t\right)\; r^{*}\left(t\right)\; dt \\ & + \int_{-\infty}^{\infty} \phi_0\left(-t\right)\; r\left(t\right)\; dt \;+\; 1\end{aligned} \tag{3.50}$$

where

$$\begin{aligned}k_2\left(t,\tau\right) \;=\; & \sum_{m=-\infty}^{0} \phi_0\left(mT-\tau\right)\; \phi_0^{*}\left(mT-t\right) \\ & + \sum_{i=1}^{\infty}\sum_{m=-\infty}^{\infty} \phi_i\left(mT-\tau\right)\; \phi_i^{*}\left(mT-t\right) \\ & + N_0\delta\left(t-\tau\right)\end{aligned} \tag{3.51}$$

Notice that $k_2(t,\tau)$ is similar to $k(t,\tau)$ from the linear equalizer analysis (equation 3.5) except that the terms involving $\phi_0(t)$ are a one-sided summation.

The problem is to find $r(t)$ which minimizes the MSE given in equation (3.50), and by the calculus of variations (see appendix A) the optimal function for $r(t)$, call it $r_o(t)$, satisfies the following integral equation:

$$\int_{-\infty}^{\infty} k_2(t,\tau)\; r_o(\tau)\; d\tau \;=\; \phi_0^*(-t) \tag{3.52}$$

The previously mentioned equation (3.7) for the optimal MSE also applies here.

Expanding the integral in equation (3.52) and grouping all integrals over $d\tau$ into constants which are not functions of t and rearranging gives the form of the optimal DFE forward filter (provided $N_0 \neq 0$):

$$\begin{aligned} r_o(t) \;=\; & \sum_{n=-\infty}^{0} a_{n_0}\; \phi_0^*(nT-t) \\ & + \sum_{i=1}^{\infty} \sum_{n=-\infty}^{\infty} a_{n_i}\; \phi_i^*(nT-t) \end{aligned} \tag{3.53}$$

where

$$a_{n_i} \;=\; \begin{cases} -\frac{U_{n_0}}{N_0} & ,i=0,\;\; n<0 \\ \frac{(1-U_{0_0})}{N_0} & ,i=0,\;\; n=0 \\ -\frac{U_{n_i}}{N_0} & ,i\neq 0,\;\; \forall n \end{cases} \tag{3.54}$$

and

$$U_{n_i} \;=\; \int_{-\infty}^{\infty} \phi_i(nT-\tau)\; r_o(\tau)\; d\tau \tag{3.55}$$

The form of equation (3.53) indicates that the optimal forward filter can be interpreted as a bank of filters matched to the individual $\{\phi_i(t)\}$ as shown Figure 3.13 with the important difference from the linear equalizer case that the synchronous filter following the matched filter $\phi_0^*(-t)$ is anti-causal. Note that for the case of just additive white noise in the channel (all interferers zero), Figure 3.13 reverts to the familiar form of a

matched filter followed by an anti-causal synchronous equalizer which minimizes the MSE of the precursor ISI.

The integral equation (3.52) for $r_o(t)$ remains to be solved.

Taking Fourier transforms of equation (3.52), gives the following:

$$\begin{aligned} N_0 R_o(f) + \Phi_0^*(f) \left[\frac{1}{T}\sum_{l=-\infty}^{\infty} \Phi_0\left(f+\frac{l}{T}\right) R_o\left(f+\frac{l}{T}\right)\right]_- \\ + \sum_{i=1}^{\infty} \Phi_i^*(f) \left[\frac{1}{T}\sum_{l=-\infty}^{\infty} \Phi_i\left(f+\frac{l}{T}\right) R_o\left(f+\frac{l}{T}\right)\right] = \Phi_0^*(f) \end{aligned} \tag{3.56}$$

Notice the similarities to equation (3.9). The presence of the third term on the left side of equation (3.56) indicates the presence of cyclostationary interferers instead of just white noise in the channel. The presence of the anti-causal operator, $[\ ]_-$, indicates that this is the equation for the DFE instead of the linear equalizer. The anti-causal operator is defined in Appendix B. Due to the presence of the anti-causal operator, the solution of equation (3.56), will have to proceed differently from the linear case.

Replace f by $f + \frac{k}{T}$ in equation (3.56) where k is any integer, rearranging and shifting an index of summation gives:

$$\Phi_0^*\left(f+\frac{k}{T}\right) [U_{0_T}(f)]_- + \sum_{m=-\infty}^{\infty} W_{k,m}(f)\, R_o\left(f+\frac{m}{T}\right) = \Phi_0^*\left(f+\frac{k}{T}\right) \tag{3.57}$$

where

$$U_{0_T}(f) = \frac{1}{T}\sum_{l=-\infty}^{\infty} \Phi_0\left(f+\frac{l}{T}\right) R_o\left(f+\frac{l}{T}\right) \tag{3.58}$$

and

$$\begin{aligned} W_{n,m}(f) &= N_0\delta_{n-m} + \sum_{i=1}^{\infty} \Phi_i^*\left(f+\frac{n}{T}\right) \Phi_i\left(f+\frac{m}{T}\right) \\ \delta_l &= \begin{cases} 1 & , l=0 \\ 0 & , l\neq 0 \end{cases} \end{aligned} \tag{3.59}$$

The subscript T in a frequency response such as $U_{0_T}(f)$ is used to indicate that it is part of a DTPF (discrete-time periodic-frequency) Fourier transform pair with period in the frequency domain being $\frac{1}{T}$. The DTPF Fourier transform is described in Appendix B. Equation (3.57) represents and infinite number of equations in k.

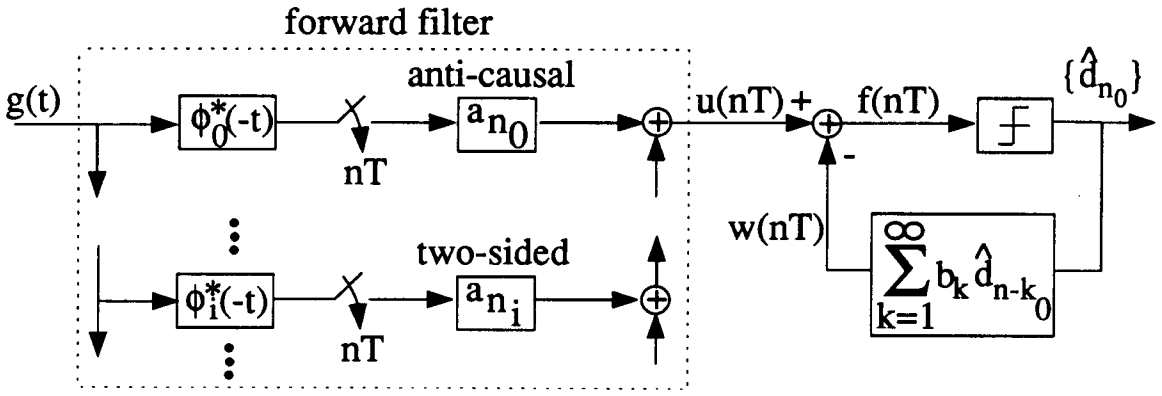

Figure 3.13 Form of the Minimum MSE Decision-Feedback Equalizer

However, if the overall channel and co-channels, $\{\Phi_i(f), i \geq 0\}$, are strictly bandlimited to $\frac{K}{2T}$, then equation (3.57) reduces to a set of $2K-1$ equations for $\{-(K-1) \leq k \leq (K-1)\}$ which can be written in matrix form in the specified frequency range as:

$$\begin{aligned} \mathbf{\Phi}_0^*(f)\ [U_{0_T}(f)]_- \ + \ \mathbf{W}(f)\ \mathbf{R_o}(f) \ &= \ \mathbf{\Phi}_0^*(f) \\ |f| &< \frac{K}{2T} \end{aligned} \tag{3.60}$$

where

$$\mathbf{\Phi}_0^*(f) = \begin{bmatrix} \Phi_0^*\left(f - \frac{K-1}{T}\right) \\ \vdots \\ \Phi_0^*\left(f - \frac{1}{T}\right) \\ \Phi_0^*(f) \\ \Phi_0^*\left(f + \frac{1}{T}\right) \\ \vdots \\ \Phi_0^*\left(f + \frac{K-1}{T}\right) \end{bmatrix}, \quad \mathbf{R_o}(f) = \begin{bmatrix} R_o\left(f - \frac{K-1}{T}\right) \\ \vdots \\ R_o\left(f - \frac{1}{T}\right) \\ R_o(f) \\ R_o\left(f + \frac{1}{T}\right) \\ \vdots \\ R_o\left(f + \frac{K-1}{T}\right) \end{bmatrix} \tag{3.61}$$

and

$$\mathbf{W}(f) = \begin{bmatrix} W_{-(K-1),-(K-1)}(f) & \cdots & W_{-(K-1),+(K-1)}(f) \\ \vdots & \ddots & \vdots \\ W_{+(K-1),-(K-1)}(f) & \cdots & W_{+(K-1),+(K-1)}(f) \end{bmatrix} \tag{3.62}$$

Solve equation (3.60) for $\mathbf{R_o}(f)$, by inverting matrix $\mathbf{W}(f)$, then premultiply both sides of the equation by $\frac{1}{T}\mathbf{\Phi}_0'(f)$ (where $'$ denotes transpose) to get:

$$U_{0_T}(f) \ = \ M_T(f)\ \left(1 - [U_{0_T}(f)]_-\right) \tag{3.63}$$

where

$$U_{0_T}(f) \ = \ \frac{1}{T}\ \mathbf{\Phi}_0'(f)\ \mathbf{R_o}(f) \tag{3.64}$$

and

$$M_T(f) \ = \ \frac{1}{T}\ \mathbf{\Phi}_0'(f)\ \ \mathbf{W}^{-1}(f)\ \ \mathbf{\Phi}_0^*(f) \tag{3.65}$$

$M_T(f)$ is real and non-negative for all frequencies; thus it has the form of a power spectrum.

Equation (3.63) may be solved for $U_{0_T}(f)$ by spectral factorization [37, 38, 39] of $1 + M_T(f)$ into causal and anti-causal components that satisfy:

$$\begin{aligned} 1 + M_T(f) &= Z_T^+(f)\ Z_T^-(f) \\ \delta_n + M_n &= Z_n^+ \star Z_n^- \\ Z_T^{+^*}(f) &= Z_T^-(f) \end{aligned} \tag{3.66}$$

and by breaking $U_{0_T}(f)$ into the following components (See Appendix B):

$$U_{0_T}(f) = [U_{0_T}(f)]_- + [U_{0_T}(f)]_{++} \tag{3.67}$$

to get:

$$Z_T^-(f)\ [U_{0_T}(f)]_- = Z_T^-(f) - \frac{1}{Z_T^+(f)} - \frac{1}{Z_T^+(f)}[U_{0_T}(f)]_{++} \tag{3.68}$$

Apply the anti-causal operator, $[\ ]_-$, to both sides of this equation and using property 6 in Appendix B to observe that the last term on the right-hand side is zero gives:

$$Z_T^-(f)\ [U_{0_T}(f)]_- = Z_T^-(f) - \left[\frac{1}{Z_T^+(f)}\right]_- \tag{3.69}$$

or:

$$[U_{0_T}(f)]_- = 1 - \frac{1}{Z_T^-(f)}\left[\frac{1}{Z_T^+(f)}\right]_- \tag{3.70}$$

Substitute $[U_{0_T}(f)]_-$ from equation (3.70) into equation (3.60) and solve for $\mathbf{R_o}(f)$ to get:

$$\mathbf{R_o}(f) = \mathbf{W}^{-1}(f)\ \mathbf{\Phi_0^*}(f)\ \frac{1}{Z_T^-(f)}\ \left[\frac{1}{Z_T^+(f)}\right]_- \tag{3.71}$$

from which $R_o(f)$ may be taken from the middle row of $\mathbf{R_o}(f)$.

The MSE can be obtained from equation (3.7) but it can be shown that a better formula exists, based on the analysis in [35]:

$$\begin{aligned} \varepsilon_{\min} &= e^{-\langle \ln(1+M_T(f)) \rangle} \\ \langle \bullet \rangle &= T \int_{-\frac{1}{2T}}^{+\frac{1}{2T}} [\bullet]\ df \end{aligned} \tag{3.72}$$

There are some properties about the optimal MSE DFE that can be discussed. First, as with the linear equalizer, the DFE is time-invariant. Second, the forward filter of the DFE acts to cause the folded equalized channel to be at or close to zero at the sampling points before the time origin and at or near one at the time origin [40]. The folded equalized channel to the right of the time origin is not relevant to the forward filter because the feedback part of the DFE subtracts off the remaining intersymbol interference. This is the same as the additive white noise case. However, in the presence of interferers, the forward-filter also acts to make the folded equalized co-channel at or near zero for all sampling points. Thus the minimum MSE for the DFE in general has the following form:

$$\varepsilon = \sigma^2_{data\ bias} + \sigma^2_{ISI\_} + \sigma^2_{Xtalk} + \sigma^2_{noise} \tag{3.73}$$

where the symbols have the same meaning as in equation 3.32 except that $\sigma^2_{ISI\_}$ is the anti-causal part of the intersymbol interference in the channel.

Chapter 4

Application of Theory

4.1 Subscriber Loop Model

The model of the subscriber loop system used to demonstrate the differences between equalization in cyclostationary interference and stationary noise is shown in Figure 4.1. Currently a single interferer is modelled but using the analysis of chapter 3, a system with multiple interferers can be modelled. The overall channel, $\Phi_0(f)$, is shown divided into the transmitted pulse, $butter1(f)$, and channel frequency response, $loop9(f)$. The overall co-channel, $\Phi_1(f)$, is shown divided into the transmitted pulse, $butter1(f)$, and co-channel frequency response, $next(f,\tau)$. The parameter $\tau \epsilon [0,T]$ represents the relative phase (a delay) of the interference with respect to the transmitted signal (as in the pedagogical example).

4.1.1 Minimum Phase Pulse

The pulse filter has a frequency response that was obtained by doing a bilinear transform [41] of a Butterworth filter. The frequency and impulse responses are shown in Figures 4.2a and 4.2b, respectively. A Butterworth filter was chosen because when sampled at the Nyquist frequency it is minimum phase. Also it allowed the pulse to be interpreted in continuous-time and bandlimited to $\frac{1}{T}$. The pulses are transmitted at a baud rate of $\frac{1}{T} = 80\ kHz$.

4.1.2 Channel Model

The channel used was Bellcore Loop #9 [42] as shown in Figure 4.3. The channel shows three bridged taps and although not shown it includes hybrid transformers and terminations at both ends. Its frequency response[9], $loop9(f)$, and impulse response, $loop9(t)$, are shown in Figures 4.4a and 4.4b, respectively.

[9] The frequency response is shown truncated to $|f| < \frac{1}{T}$ only because the pulse, $butter1(f)$, is strictly bandlimited to $\frac{1}{T}$.

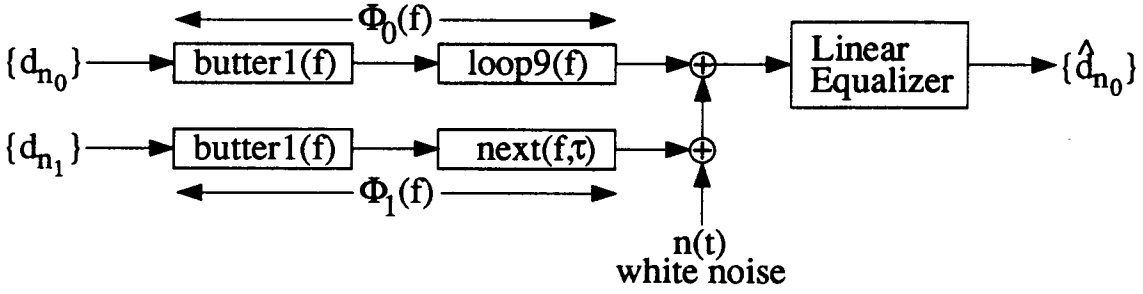

Figure 4.1 Subscriber Loop Model

[a]

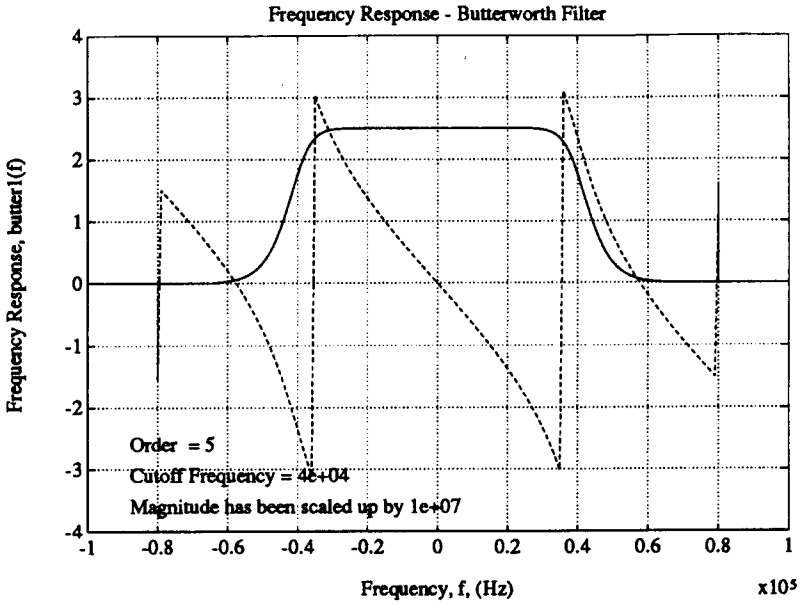

[b]

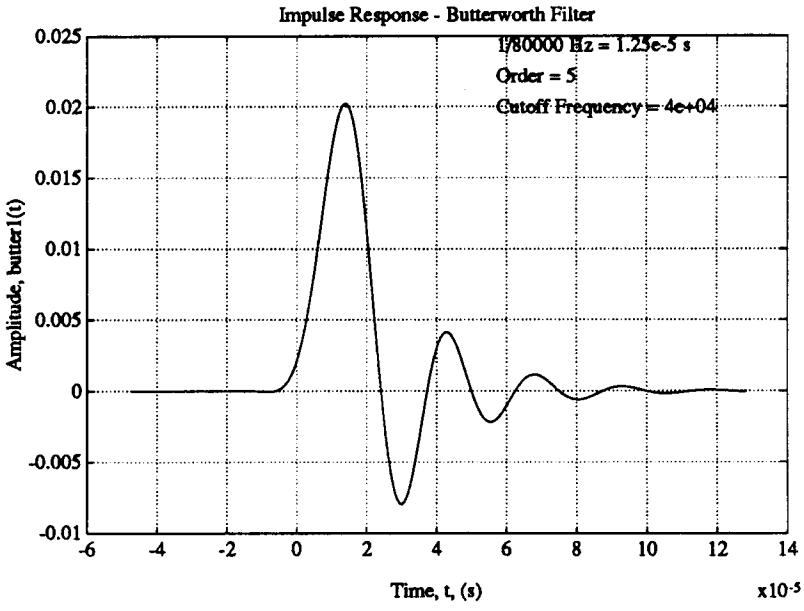

Figure 4.2 Pulse Shape Frequency and Impulse Responses

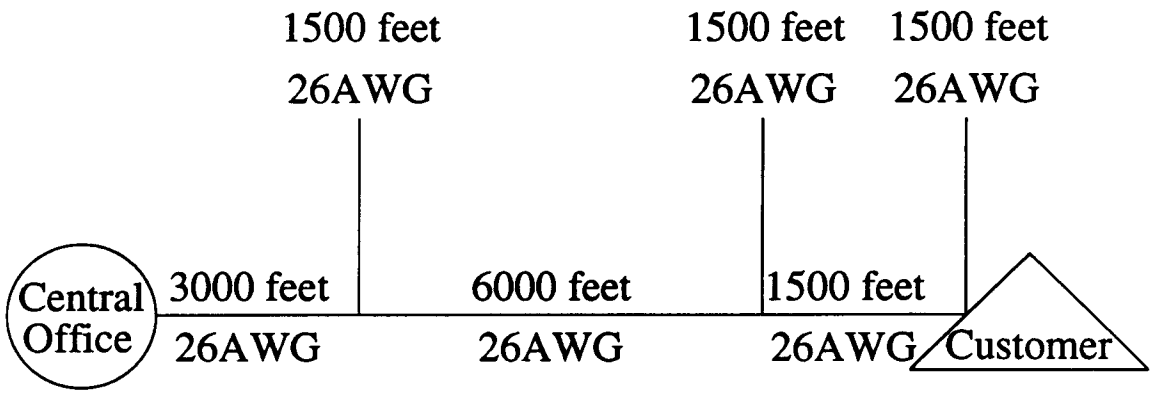

Figure 4.3 Bellcore Loop #9

[a]

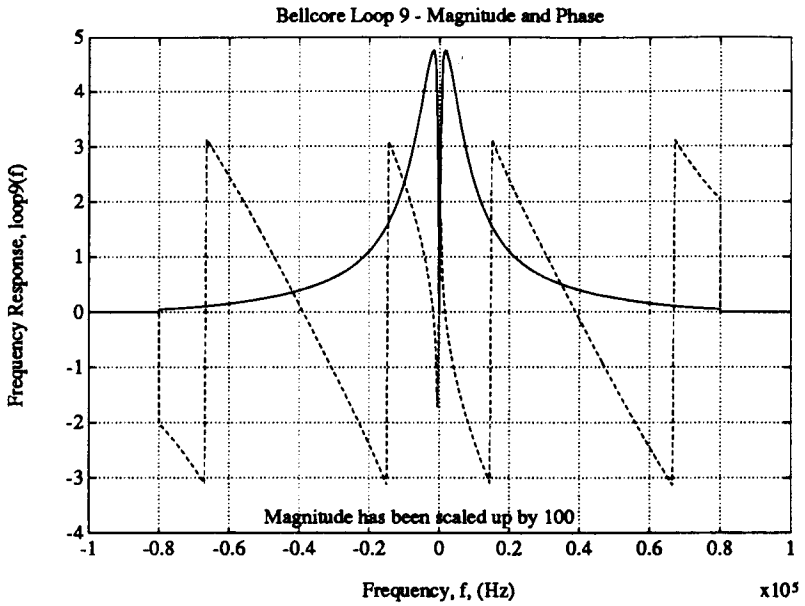

[b]

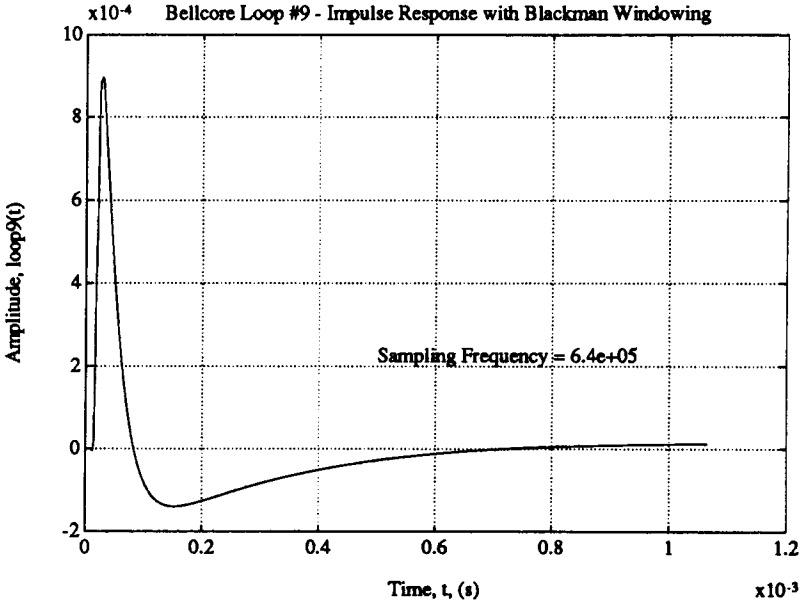

Figure 4.4 Bellcore Loop #9 Frequency and Impulse Responses

From the pulse, $butter1\ (f)$, and the channel, $loop9\ (f)$, the overall channel, $\Phi_0\ (f)$ can be determined and its frequency and impulse responses are shown in Figures 4.5a and 4.5b, respectively.

The power spectrum of the white noise is: $N_0 = 3.75 \times 10^{-18}\ \frac{W}{Hz}$.

4.1.3 Co-channel Model

The dominant form of co-channel interference in subscriber loops is near-end crosstalk (NEXT) resulting from interferers on the same side of the network. Far-end crosstalk (FEXT) does not dominate because the subscriber loops attenuate the far-end signal and far-end crosstalk. The NEXT is modelled here by [2]:

$$|next\ (f)|^2 = \frac{K}{2}\ f^{\frac{3}{2}} \tag{4.1}$$

$$K = 10^{-13} \tag{4.2}$$

where f is two-sided and measured in Hz and $|next\ (f)|^2$ is measured in $\frac{W}{Hz}$. The choice of K is to provide a reasonable upper bound (worst case) NEXT power [42]. The parameter for delay, τ, will be added at the end of the development of the model. This model only includes the magnitude response, so minimum phase was assumed in order to make the energy of the interference impulse response causal and concentrated about the time origin [41, 43].

The NEXT model will be of the form:

$$next\ (f) = |next\ (f)|\ e^{j\ Arg\ (next\ (f))} \tag{4.3}$$

where

$$|next\ (f)| = \sqrt{\frac{K}{2}\ f^{\frac{3}{2}}} \tag{4.4}$$

is known. $Arg\ (next\ (f))$ is unknown but can be determined since signals which satisfy the following Hilbert transform pair are minimum phase [41, 44]:

$$\begin{aligned} Arg\ (next\ (f)) &= \mathcal{H}\{log_e\ |next\ (f)|\} \\ log_e\ |next\ (f)| &= -\mathcal{H}\{Arg\ (next\ (f))\} \end{aligned} \tag{4.5}$$

[a]

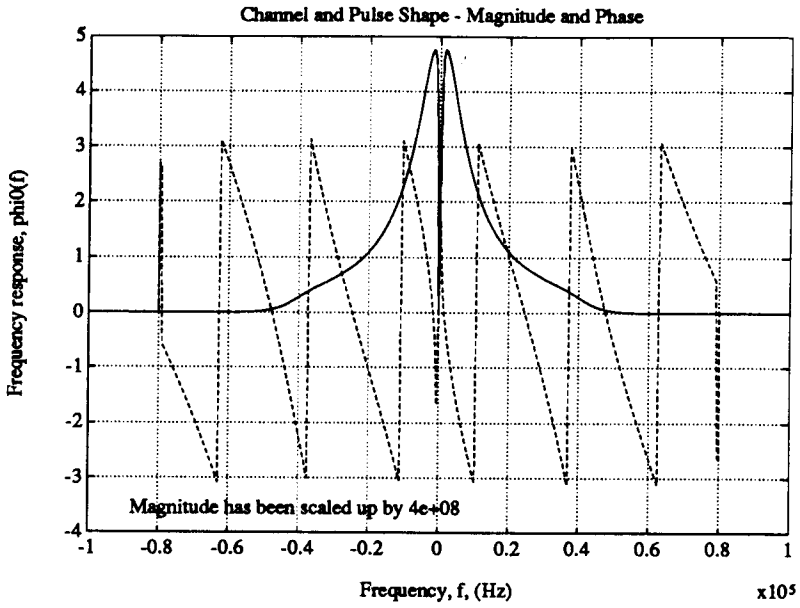

[b]

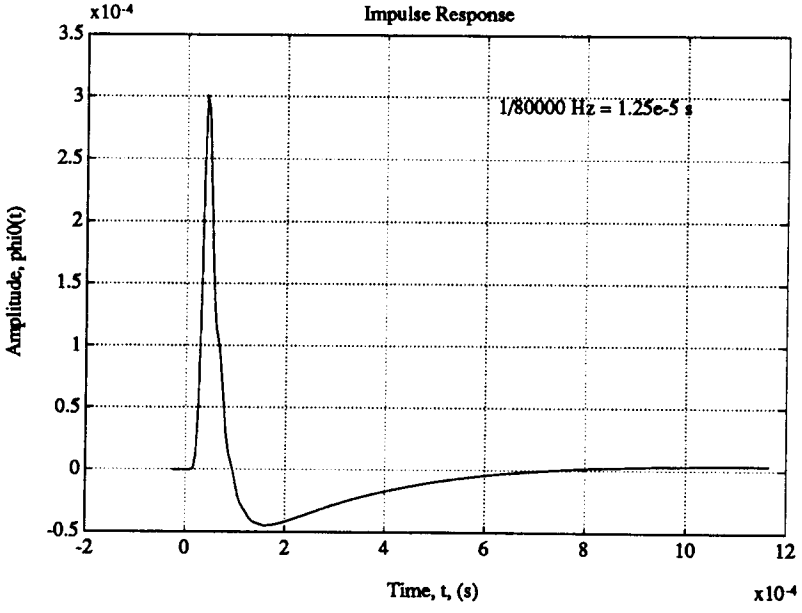

Figure 4.5 Overall Channel Frequency and Impulse Responses

where

$$\mathcal{H}\{f(t)\} = \frac{1}{\pi}\int_{-\infty}^{\infty}\frac{f(\tau)}{t-\tau}\,d\tau \tag{4.6}$$

It was found that:

$$\begin{aligned} Arg\,(next\,(f)) &= -\frac{3}{8}\pi\; sgn\,(f) \\ sgn\,(f) &= \begin{cases} -1 & ,f<0 \\ 0 & ,f=0 \\ +1 & ,f>0 \end{cases} \end{aligned} \tag{4.7}$$

Adding the delay component associated with τ, the NEXT model is the same as the interference model shown previously in the pedagogical example in equation (3.20).

The frequency response of $next(f,\tau)$ is shown in Figure 4.6. Since $next(f,\tau)$ is multiplied by the bandlimited pulse $butter1\,(f)$ it is only shown for the bandwidth of interest.

From the pulse, $butter1\,(f)$, and the co-channel, $next\,(f,\tau)$, the overall co-channel, $\Phi_1(f)$ can be determined and its frequency and impulse responses are shown in Figures 4.7a and 4.7b, respectively.

Using these signal and NEXT models, the cyclostationarity versus time (see the form of equation 2.8) of the signal, and the interference with bandlimited noise at the input to the linear equalizer were determined and they are shown in Figures 4.8a and 4.8b, respectively (Note that the baud rate is 80 kHz).

In a more elaborate model of the interference [1], the degree of cyclostationarity drops as the baud rate is increased. This same effect was also demonstrated in [15] where using a finite-length discrete-time DFE in cyclostationary interference showed performance gains that were lower at a baud rate of 400 kHz compared to 80 kHz; however the interference model used in that work was obtained from measurements. Similar measurements as in [15] will be used in future work; these measurements have recently been taken [13].

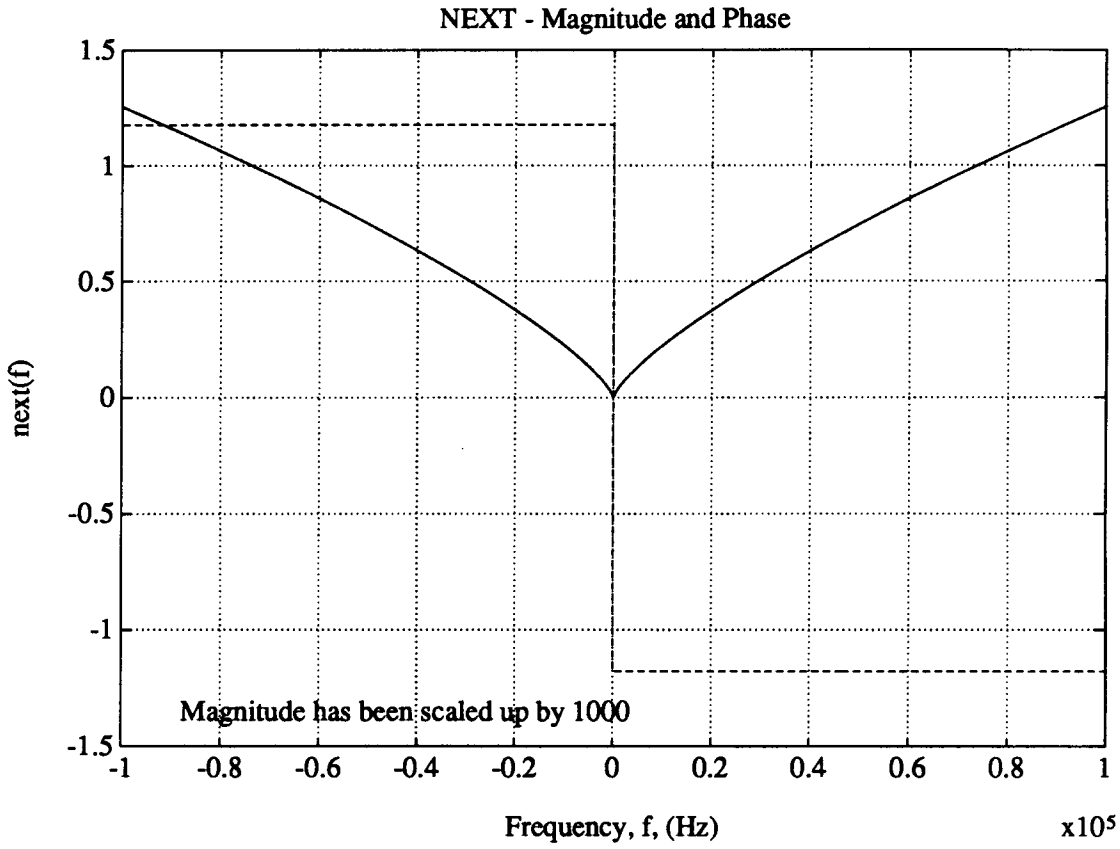

Figure 4.6 Minimum Phase Interference Frequency Response

[a]

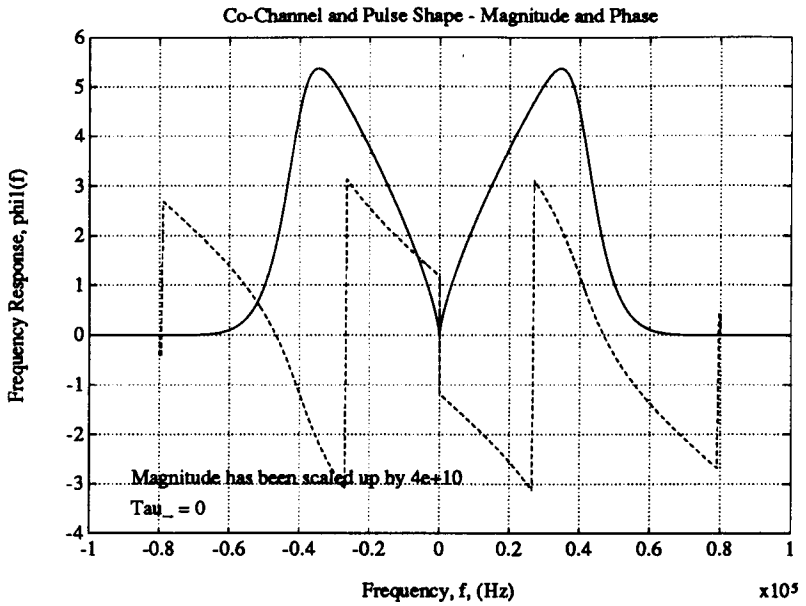

[b]

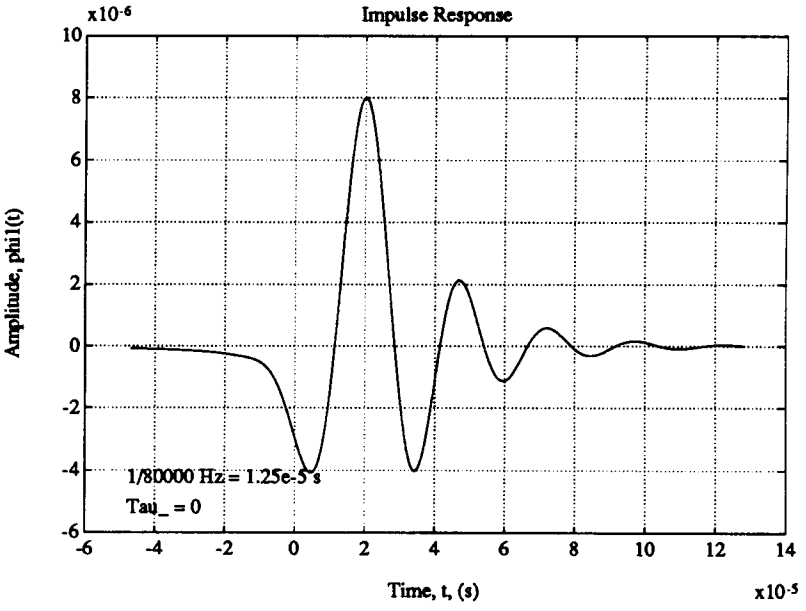

Figure 4.7 Overall Co-channel Frequency and Impulse Responses

[a]

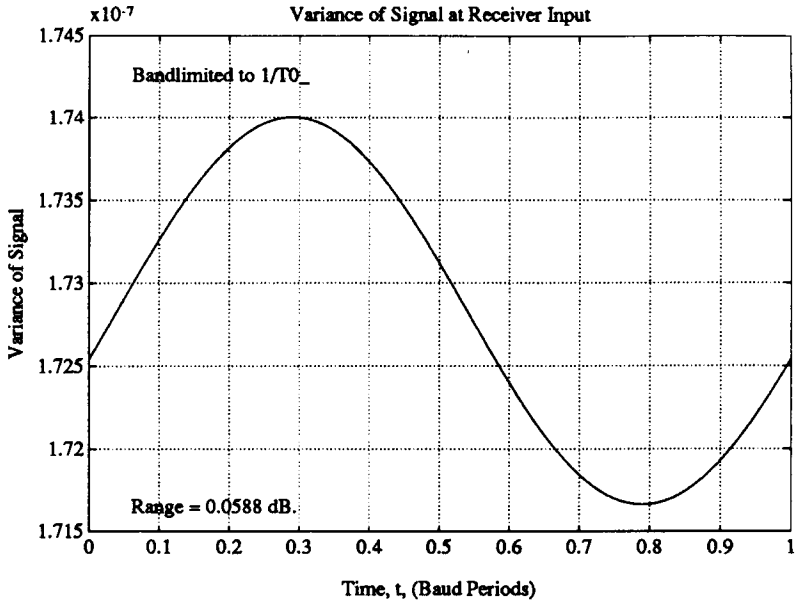

[b]

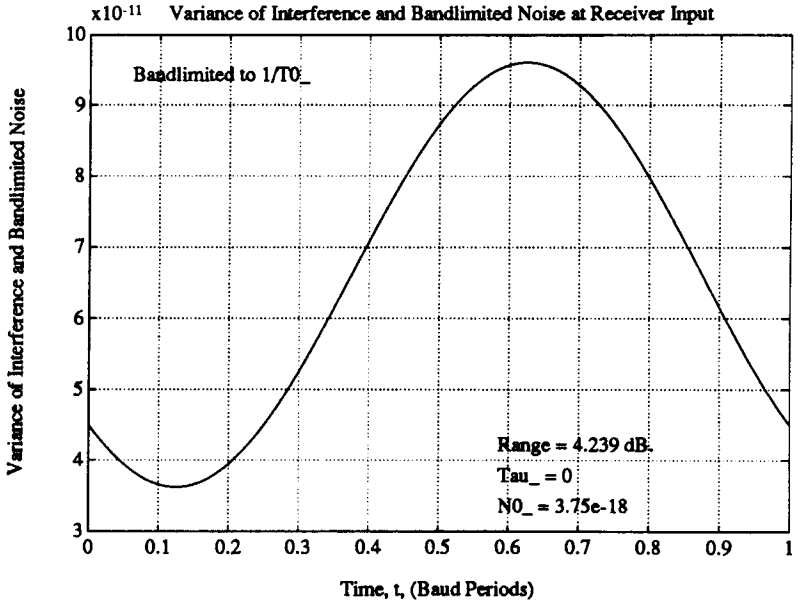

Figure 4.8 Degree of Cyclostationarities

4.2 Linear Equalizer Results

For the subscriber loop system shown in Figure 4.1, the $SINR$ is 34.2 dB, the SIR is 34.2 dB and the SNR is 54.6 dB.

The MSE (see equation 3.7) with respect to the relative phase of the single interferer is plotted in Figure 4.9.

At at relative interference phase of $\tau = 0$, the optimal cyclostationary and stationary linear equalizer frequency responses were plotted in Figures 4.10a and 4.10b using equations 3.11 and 3.15, respectively; their corresponding impulse responses are shown in Figures 4.11a and 4.11b, respectively.

The sampled equalized channel frequency response for the cyclostationary and stationary cases are plotted in Figures 4.12a and 4.12b, respectively; their corresponding impulse responses are shown in Figures 4.13a and 4.13b, respectively.

The sampled equalized co-channel frequency response for the cyclostationary case is plotted in Figure 4.14a; the corresponding impulse response is shown in Figure 4.14b. Note that this information for the stationary linear equalizer is not meaningful since it is not concerned with co-channel interference suppression.

These results deserve further comment. In Figure 4.9 there is roughly between 4 dB and 9 dB difference in MSE performance between the cyclostationary and stationary cases. This large difference is due to there being only one interferer as well as signal and interference bandwidths up to $\frac{1}{T}$. Under these conditions, in general it is likely that in the absence of noise that the interference can be completely suppressed (see the zero-forcing equalizer analysis). So that in this situation, the linear equalizer has sufficient flexibility regarding the components of the MSE that need to be suppressed that the performance is limited by the amount of white noise. If however, more than one interferer was modelled as in more realistic situations, then the performance would probably not be limited by the white noise, but instead by the interference.

Notice in Figure 4.13 that for both the cyclostationary and stationary cases, as predicted, the sampled equalized channel (sampled at T-spaced intervals) passes through

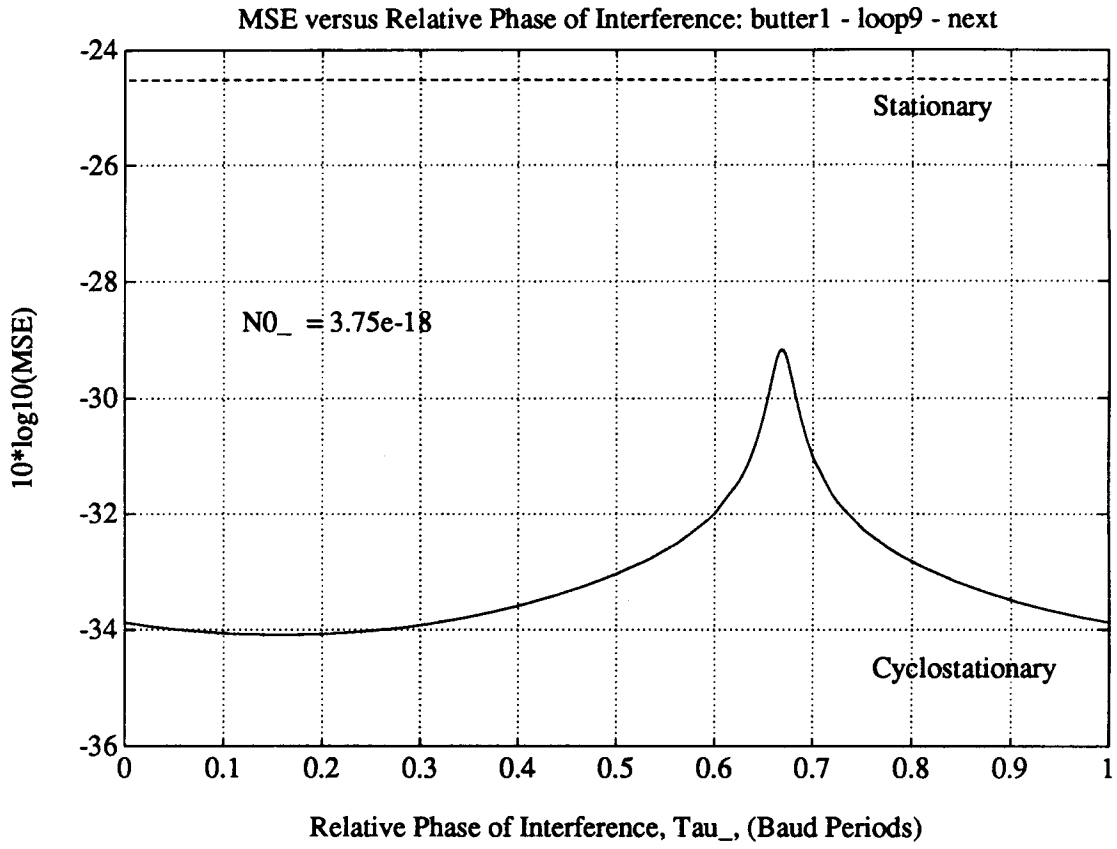

Figure 4.9 MSE versus Relative Phase of Interference

[a]

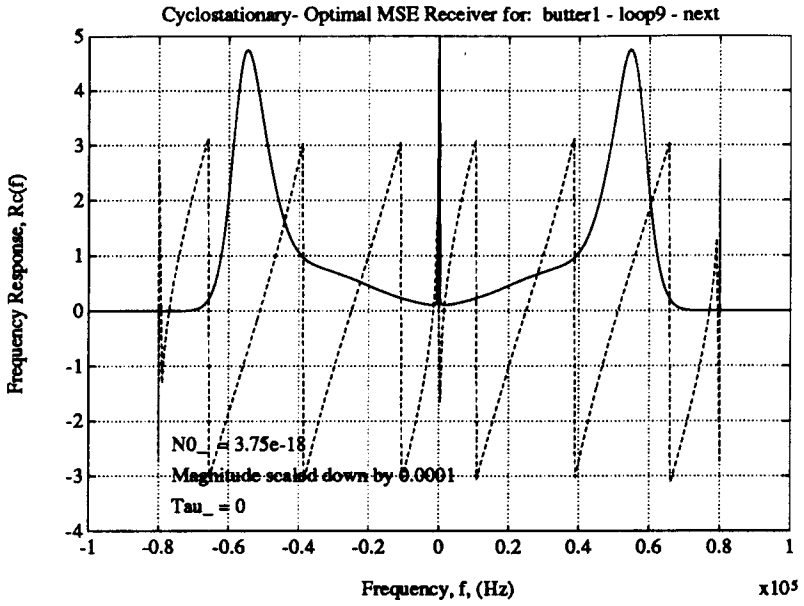

[b]

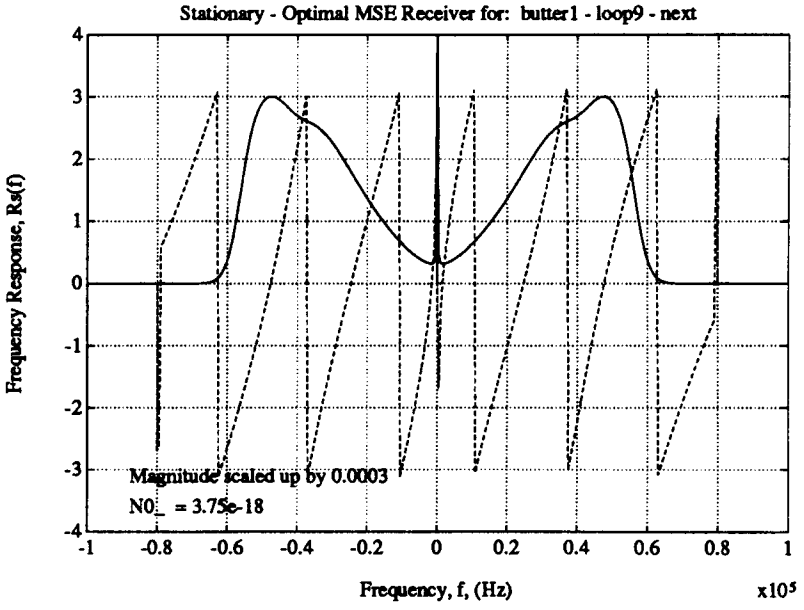

Figure 4.10 Optimal Linear Equalizers - Frequency Responses

[a]

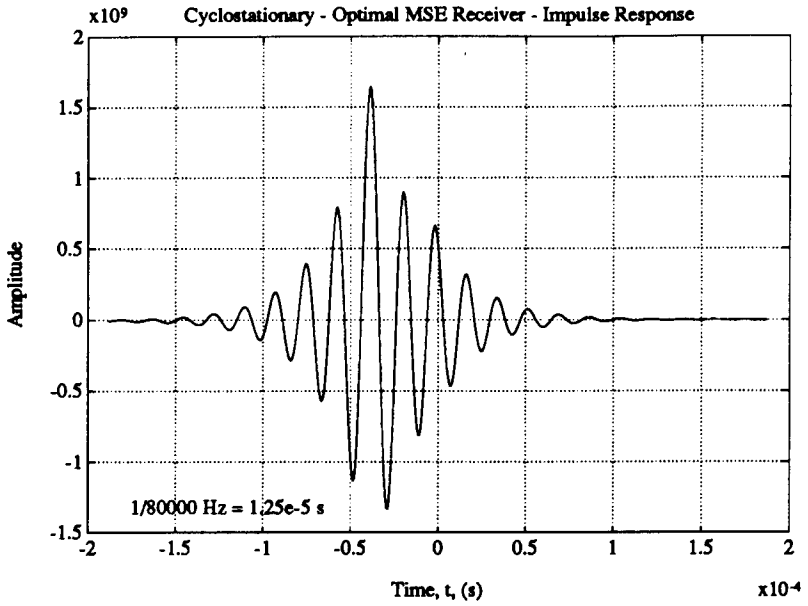

[b]

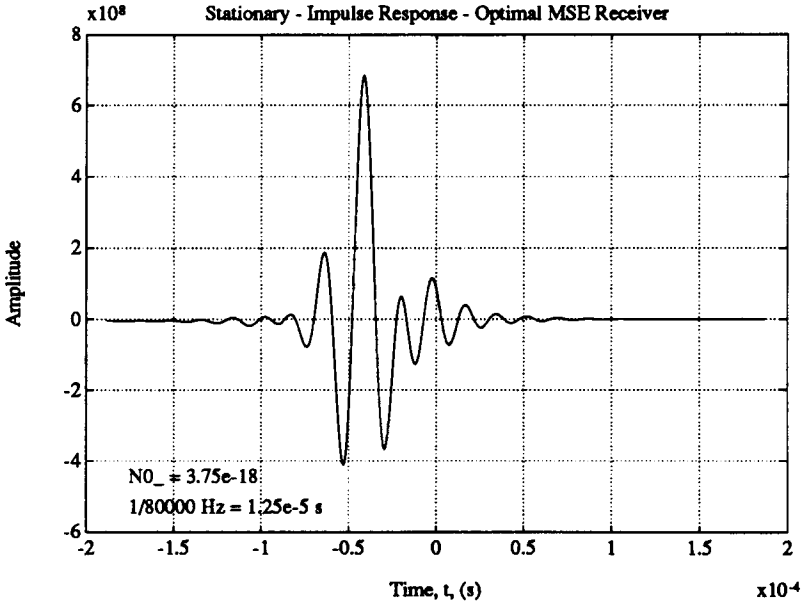

Figure 4.11 Optimal Linear Equalizers - Impulse Responses

[a]

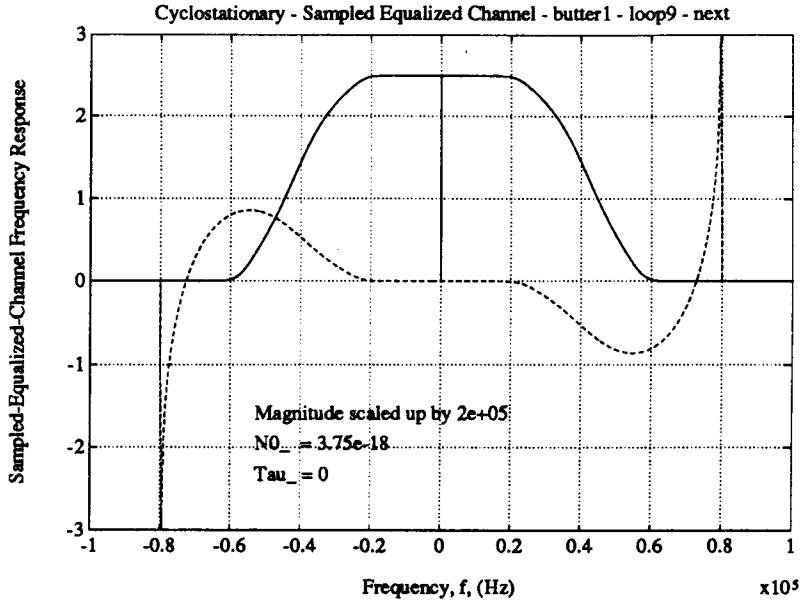

[b]

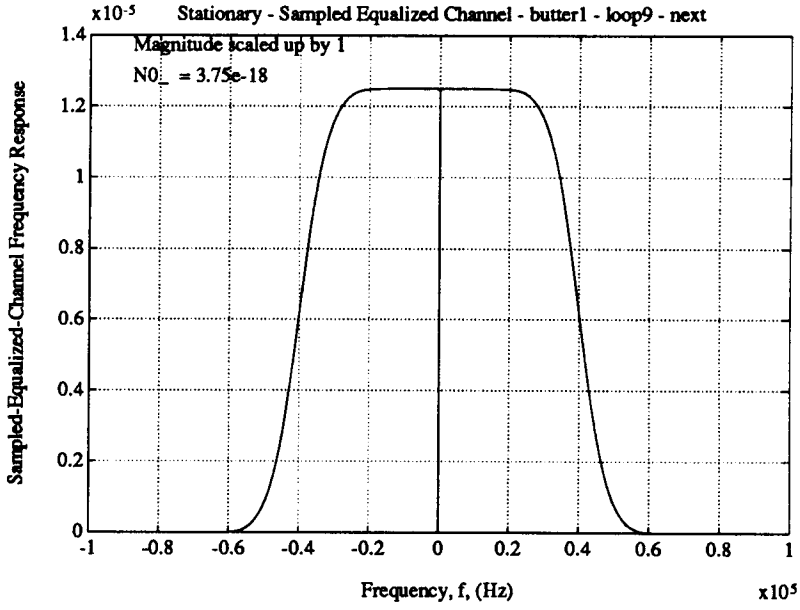

Figure 4.12 Sampled Equalized Channels - Frequency Responses

[a]

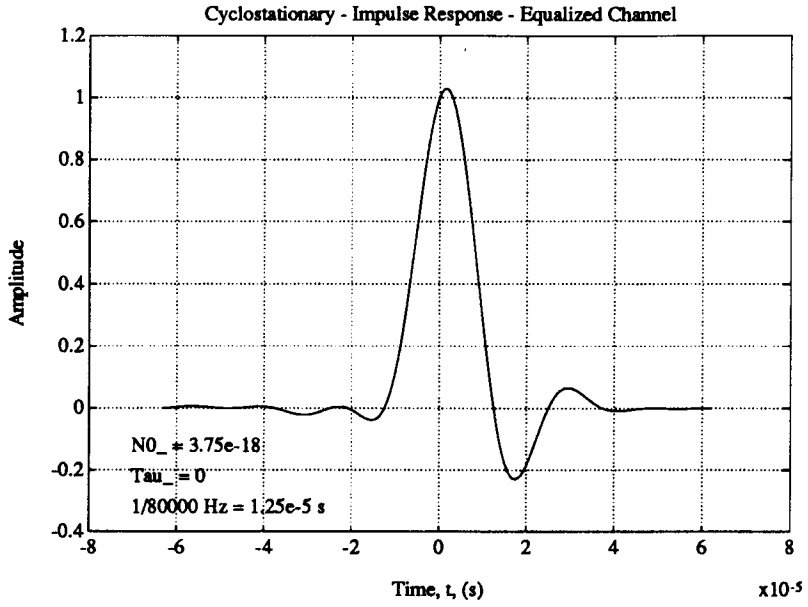

[b]

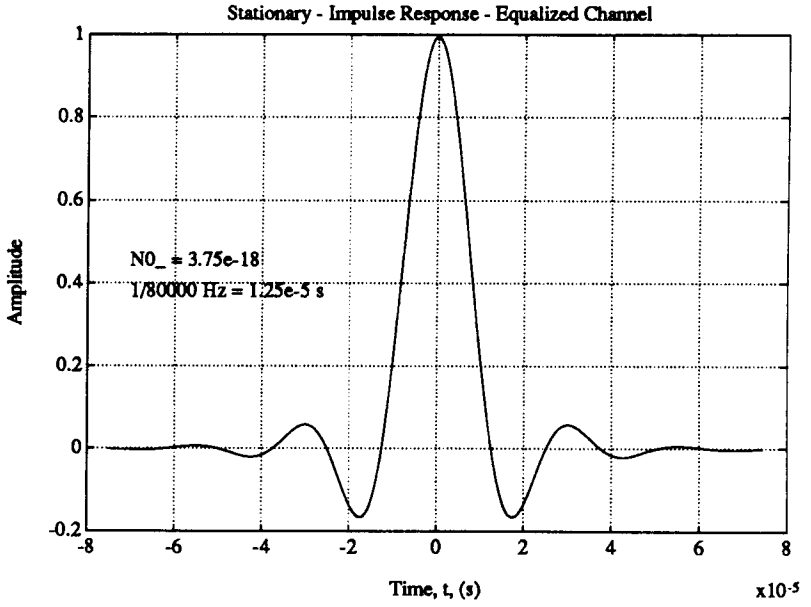

Figure 4.13 Sampled Equalized Channels - Impulse Responses

[a]

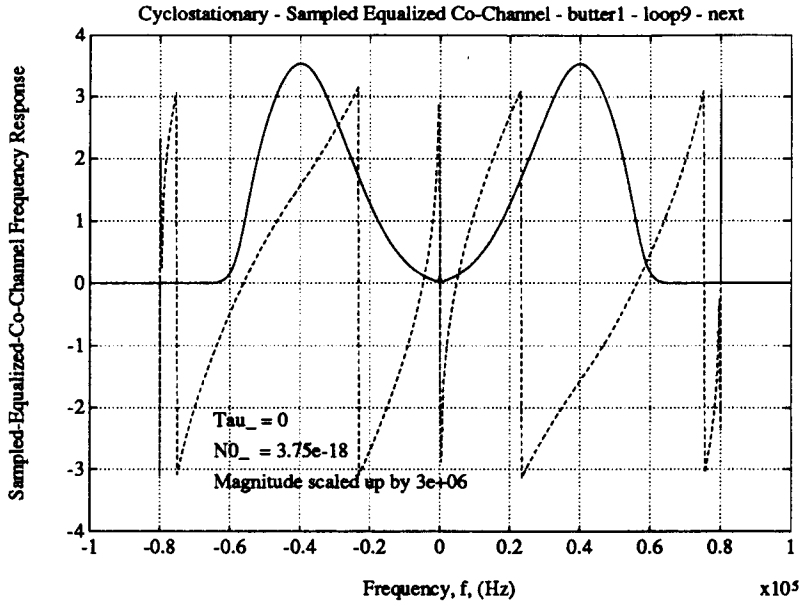

[b]

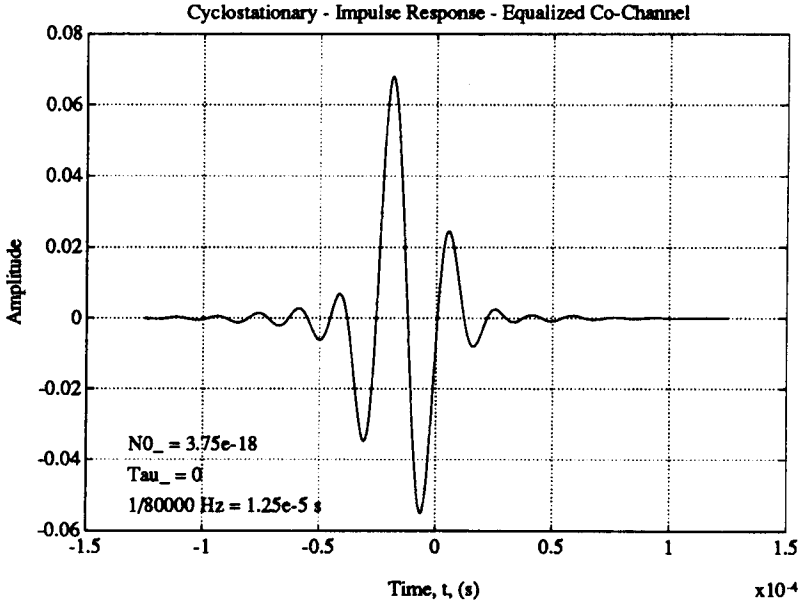

Figure 4.14 Sampled Equalized Co-Channel - Frequency and Impulse Responses

or near zero at the sampling points and through or near one at the time origin.

In Figure 4.14 the sampled equalized co-channel passes through or near zero at all the sampling points because the linear equalizer is trying to suppress the interferers. However, this is not a requirement for the stationary case.

In the case of cyclostationary interference, the performance of the equalizer will change with the introduction of a relative shift of the interference with respect to the data carried in the channel. For the bounds presented here, there will be no change in linear equalizer performance with respect to the receiver sampling phase[10] in the case where the sampling phase is set before the MSE minimization. This is because a continuous-time linear equalizer can synthesize a perfect delay.

A more complete model of the interference would include multiple interferers with some relative difference in phases with respect to each other. A more realistic model of a subscriber loop cable bundle would have a smaller difference in the performance in cyclostationary and stationary interference. Measurements of cyclostationary interference have been carried out [13]. However, the results shown here do indicate that the cyclostationary nature of the interference can be exploited in equalization. The results also indicate the advantage of deliberately synchronizing the transmitters at the central office.

---

[10] Recall for the continuous-time linear equalizer, the sampler follows the continuous-time filter.

Chapter 5

Summary

Analysis of the performance of continuous-time minimum mean-square error linear, zero-forcing and decision-feedback equalizers in the presence of cyclostationary interference have been carried out and are nearly completed. It was shown that when the interference is not bandlimited to $\frac{1}{2T}$ that the receivers for the two cases differ significantly. It was also shown that if the overall channel and co-channels have a bandwidth greater than or equal to $\frac{K}{2T}$ that there is sufficient flexibility to completely suppress $K-1$ interferers. For comparison, the performance of the linear equalizer in stationary noise having the same mean power spectrum as the cyclostationary interference was determined. The comparisons were taken further in an application to a digital subscriber loop system. It showed the cyclostationarity of the interference can be exploited in equalization.

Appendix A

The Calculus of Variations Solution of the MSE Functional

Given the following functional[11] (from equations (3.4) or (3.50)):

$$\varepsilon = \int_{-\infty}^{\infty}\int_{-\infty}^{\infty} k(t,\tau)\, r(\tau)\, r^*(t)\, d\tau\, dt + \int_{-\infty}^{\infty} \phi_0^*(-t)\, r^*(t)\, dt + \int_{-\infty}^{\infty} \phi_0(-\tau)\, r(\tau)\, d\tau + 1 \tag{A.1}$$

where $k(t,\tau)$ and $\phi_0(t)$ are known, then the problem is to find the function $r(t)$ which minimizes ε.

Let $r_o(t)$ be the function which minimizes ε. Also let:

$$\begin{aligned} r(t) &= r_o(t) + \epsilon_1 n_1(t) \\ r(\tau) &= r_o(\tau) + \epsilon_2 n_2(\tau) \end{aligned} \tag{A.2}$$

where ϵ_1 and ϵ_2 are real scalars and $n_1(t)$ and $n_2(\tau)$ are arbitrary[12] complex functions. Thus ε can now be expressed as:

$$\begin{aligned} \varepsilon(\epsilon_1, \epsilon_2) = &\int_{-\infty}^{\infty}\int_{-\infty}^{\infty} k(t,\tau)\, [r_o(\tau) + \epsilon_2 n_2(\tau)]\, [r_o(t) + \epsilon_1 n_1(t)]^*\, d\tau\, dt \\ &+ \int_{-\infty}^{\infty} \phi_0^*(-t)\, [r_o(t) + \epsilon_1 n_1(t)]^*\, dt \\ &+ \int_{-\infty}^{\infty} \phi_0(-\tau)\, [r_o(\tau) + \epsilon_2 n_2(\tau)]\, d\tau + 1 \end{aligned} \tag{A.3}$$

Since $\varepsilon(\epsilon_1, \epsilon_2)$ has a global minimum at $(\epsilon_1, \epsilon_2) = (0, 0)$, the following is true:

$$\frac{\partial \varepsilon(\epsilon_1, \epsilon_2)}{\partial \epsilon_1}\Big|_{\epsilon_2=0} = 0 \tag{A.4}$$

---

[11] A functional accepts as input a function and produces as output a scalar value.

[12] These functions are chosen to be sufficiently well behaved to allow analysis; they have up to and including second order derivatives with respect to t (or τ).

A number of derivative properties of the global minimum would be true, but this one is sufficient to complete the solution. Evaluating gives:

$$\int_{-\infty}^{\infty}\int_{-\infty}^{\infty} k(t,\tau)\, r_o(\tau)\, n_1^*(t)\, d\tau\, dt \;-\; \int_{-\infty}^{\infty} \phi_0^*(-t)\, n_1^*(t)\, dt \;=\; 0$$

$$\int_{-\infty}^{\infty}\left[\int_{-\infty}^{\infty} k(t,\tau)\, r_o(\tau)\, d\tau \;-\; \phi_0^*(-t)\right] n_1^*(t)\, dt \;=\; 0 \tag{A.5}$$

But since $n_1(t)$ is arbitrary it means that [45]:

$$\int_{-\infty}^{\infty} k(t,\tau)\, r_o(\tau)\, d\tau \;-\; \phi_0^*(-t) \;=\; 0 \tag{A.6}$$

This is the equation from which $r_o(t)$ may be determined (even though it is an integral equation). In fact the problem can be interpreted as a time-*variant* deconvolution where the output of a system is known, the time-variant impulse response is known and the input is unknown.

Appendix B The Anti-Causal Operator

B.1 Definition

If the DTPF (discrete-time periodic-frequency) Fourier transforms are denoted by:

$$\begin{aligned} X_T(f) &= \mathcal{F}_{\text{DTPF}}[x_n] \\ &= \sum_{n=-\infty}^{\infty} x_n \, e^{-j2\pi nTf} \end{aligned}$$

$$\begin{aligned} x_n &= \mathcal{F}^{-1}_{\text{DTPF}}[X_T(f)] \\ &= T \int_{-\frac{1}{2T}}^{\frac{1}{2T}} X_T(f) \, e^{j2\pi fTn} \, df \end{aligned}$$

Then the anti-causal operator, $[\,]_-$, operating on $X_T(f)$ is defined as:

$$\begin{aligned} [X_T(f)]_- &\triangleq \sum_{n=-\infty}^{0} x_n \, e^{-j2\pi nTf} \\ &= \mathcal{F}_{\text{DTPF}}\left[u(-n) \;\; \mathcal{F}^{-1}_{\text{DTPF}}[X_T(f)]\right] \end{aligned}$$

$$u(n) = \begin{cases} 1 & , n \geq 0 \\ 0 & , n < 0 \end{cases}$$

The following associated definitions will be useful:

$$[X_T(f)]_{--} \triangleq \sum_{n=-\infty}^{-1} x_n \, e^{-j2\pi nTf}$$

$$[X_T(f)]_{++} \triangleq \sum_{n=1}^{\infty} x_n \, e^{-j2\pi nTf}$$

$$[X_T(f)]_{+} \triangleq \sum_{n=0}^{\infty} x_n \, e^{-j2\pi nTf}$$

Let the same notation apply to the sequences y_n and z_n to show the properties in the section to follow.

B.2 Properties

1. $[k\, X_T(f)]_- = k\, [X_T(f)]_-$
2. $[X_T(f)\, Y_T(f)]_- = [Y_T(f)\, X_T(f)]_-$
3. $[X_T(f)\, (Y_T(f) + Z_T(f))]_- = [X_T(f)\, Y_T(f)]_- + [X_T(f)\, Z_T(f)]_-$
4. $X_T(f) = [X_T(f)]_- + [X_T(f)]_{++}$
5. $X_T(f) = [X_T(f)]_{--} + [X_T(f)]_+$
6. $[\, [X_T(f)]_+ \; [Y_T(f)]_{++} \,]_- = 0$

References

[1] J. C. Campbell, A. J. Gibbs, and B. M. Smith, "The cyclostationary nature of crosstalk interference from digital signals in multipair cable-Part I: Fundamentals and Part II: Applications and further results," *IEEE Trans. on Commun.*, vol. COM-31, no. 5, pp. 629–649, May 1983.

[2] D. G. Messerschmitt, "Design issues in the ISDN U-interface transceiver," *IEEE J. Select Areas Commun.*, vol. SAC-4, no. 8, pp. 1281–1293, Nov. 1986.

[3] J. W. Lechleider, "Loop transmission aspects of ISDN basic access," *IEEE J. Select Areas Commun.*, vol. SAC-4, no. 8, pp. 1294–1301, Nov. 1986.

[4] P. Cochrane and M. Brain, "Future optical fiber transmission technology and networks," *IEEE Communications Magazine*, vol. 26, no. 11, pp. 45–60, Nov. 1988.

[5] American National Standards Institute, *Integrated services digital network (ISDN) basic access interface for use on metallic loops for application on the network side of the NT (layer 1 specification)*, ANSI T1-601-1988, Sept. 1988.

[6] G. Stix, "Telephone wiring: a conduit for networking standards," *IEEE Spectrum*, vol. 25, no. 6, pp. 38–41, June 1988.

[7] G. P. Dudevoir, J. S. Chow, J. M. Cioffi, and S. Kasturia, "Combined equalization and coding for T1 data rates on carrier serving areas subscriber loops," in *Conf. Rec. IEEE ICC 89*, vol. 1, (Boston, MA), pp. 536–540, June 11-14 1989.

[8] R. G. Hunt, J. W. Cook, K. H. Kirkby, and N. G. Cole, "The potential for high-rate digital subscriber loops," in *Conf. Rec. IEEE ICC 89*, vol. 1, (Boston, MA), pp. 520–524, June 11-14 1989.

[9] P. Mohanraj, V. Joshi, D. D. Falconer, and T. A. Kwasniewski, "Reduced-complexity trellis coding/decoding for high bit rate digital subscriber loop transmission," in *Conf. Rec. IEEE ICC 89*, vol. 1, (Boston, MA), pp. 525–530, June 11-14 1989.

[10] D. W. Lin, "High bit rate digital subscriber line transmission with noise-predicative decision feedback equalization and block coded modulation," in *Conf. Rec. IEEE ICC 89*, vol. 1, (Boston, MA), pp. 531–535, June 11-14 1989.

[11] AT&T, *Telecommunications Transmission Engineering : Volume 3 — Networks and Services*. Winston-Salen, NC: Western Electric Co. Inc. Technical Publications, AT&T Co., 1977.

[12] S. H. Lin, "Statistical behaviour of multipair crosstalk," *Bell Syst. Tech. J.*, vol. 59, no. 6, pp. 995–974, July-Aug. 1980.

[13] A. Fung, L. S. Lee, and D. D. Falconer, "A facility for near end crosstalk measurements on ISDN subscriber loops," in *Conf. Rec. IEEE Globecom 89*, vol. 3, (Dallas, TX), pp. 1592–1596, Nov. 27-30 1989.

[14] R. C. Bernhardt, "The character of co-channel interference in frequency reuse radio systems." private communication, Bell Communications Research, Inc., Red Bank, New Jersey 07701, received Mar. 29, 1989.

[15] M. Abdulrahman, "Decision-feedback equalization with cyclostationary interference for DSL," Master's thesis, Carleton University, Ottawa, ON, Canada, SCE-89-16, June, 1989.

[16] J. G. Proakis, *Digital Communications*. New York: McGraw-Hill Inc., 1983.

[17] L. E. Franks, "Carrier and bit synchronization in data communication - a tutorial review," *IEEE Trans. on Commun.*, vol. COM-28, no. 8, pp. 1107–1121, Aug. 1980.

[18] W. A. Gardner and L. E. Franks, "Characterization of cyclostationary random processes," *IEEE Trans. on Inform. Theory*, vol. IT-21, no. 1, pp. 4–14, Jan. 1975.

[19] M. Kavehrad and J. Salz, "Cross-polarization cancellation and equalization in digital transmission over dually polarized multipath fading channels," *AT&T Tech. J.*, vol. 64, no. 10, pp. 2211–2245, Dec. 1985.

[20] M. L. Honig and D. G. Messerschmitt, *Adaptive Filters: Structures, Algorithms and Applications*. Hingham, MA: Kluwer Academic Publishers, 1984.

[21] S. U. H. Qureshi, "Adaptive equalization," *Proc. IEEE*, vol. 73, no. 9, pp. 1349–1387, Sept. 1985.

[22] S. Haykin, *Adaptive Filter Theory*. Englewood Cliffs, New Jersey: Prentice-Hall, 1986.

[23] R. D. Gitlin and S. B. Weinstein, "Fractionally-spaced equalization: an improved digital transversal filter," *Bell Syst. Tech. J.*, vol. 60, no. 2, pp. 275–296, Jan. 1981.

[24] P. Crespo, M. L. Honig, and K. Steiglitz, "Optimization of pre- and post- filters in the presence of near- and far- end crosstalk," in *Conf. Rec. IEEE ICC 89*, vol. 1, (Boston, MA), pp. 541–547, June 11-14 1989.

[25] P. Crespo, M. L. Honig, and K. Steiglitz, "Optimization of pre- and post- filters in the presence of near- and far- end crosstalk." private communication, Bell Communications Research, Inc., 445 South Street, Morristown, New Jersey 07960-1910, received Sept. 26, 1989.

[26] J. H. Winters, "Optimum combining in digital mobile radio with cochannel interference," *IEEE J. Select Areas Commun.*, vol. SAC-2, no. 4, pp. 528–539, July 1984.

[27] J. Salz, "Digital transmission over cross-coupled linear channels," *AT&T Tech. J.*, vol. 64, no. 6, pp. 1147–1159, July-Aug. 1985.

[28] N. Amitay and J. Salz, "Linear equalization theory in digital data transmission over dually polarized fading radio channels," *AT&T Tech. J.*, vol. 63, no. 10, pp. 2215–2259, Dec. 1984.

[29] E. Biglieri, M. Elia, and L. LoPresti, "Optimal linear receiving filter for digital transmission over nonlinear channels," in *Conf. Rec. IEEE Globecom 84*, vol. 2, (Atlanta, GA), pp. 1063–1067, Nov. 26-29 1984.

[30] E. Biglieri, M. Elia, and L. LoPresti, "The optimal linear receiving filter for digital transmission over nonlinear channels," *IEEE Trans. on Inform. Theory*, vol. IT-35, no. 3, pp. 620–625, May 1989.

[31] B. R. Petersen and D. D. Falconer, "Linear equalization in cyclostationary crosstalk." submitted but not accepted April 15, 1989 to Globecom 1989, Dallas, TX, Nov., 1989.

[32] W. A. Gardner, *Introduction to Random Processes with Applications to Signals and Systems*. London: Collier Macmillan Publishers, 1986.

[33] T. Kailath, "The innovations approach to detection and estimation theory," *Proc. IEEE*, vol. 58, no. 5, pp. 680–695, May 1970.

[34] R. W. Lucky, J. Salz, and E. J. Weldon, *Principles of Data Communication*. New York: McGraw-Hill Inc., 1968.

[35] J. Salz, "Optimum mean-square decision feedback equalization," *Bell Syst. Tech. J.*, vol. 52, no. 8, pp. 1341–1373, Oct. 1973.

[36] J. Salz, "On mean-square decision feedback equalization and timing phase," *IEEE Trans. on Commun.*, vol. COM-25, no. 12, pp. 1471–1476, Dec. 1977.

[37] A. Papoulis, *Random Variables and Stochastic Processes*. New York: McGraw-Hill Book Company, 2nd ed., 1984.

[38] H. L. VanTrees, *Detection, Estimation and Modulation Theory, Part I*. New York: John Wiley & Sons Inc., 1968.

[39] H. V. Poor, *An Introduction to Detection and Estimation*. New York: Dowden & Culver Inc., 1988.

[40] R. Price, "Nonlinearly feedback-equalized PAM versus capacity for noisy filter channels," in *Conf. Rec. IEEE ICC 72*, (Philadelphia, PA), pp. 22.12–22.16, June 19-21 1972.

[41] A. V. Oppenheim and R. W. Schafer, *Digital Signal Processing*. Englewood Cliffs, NJ: Prentice-Hall, 1975.

[42] Ad Hoc Group on Draft Standard, *Draft standard for ISDN basic access interface for application at the network side of NT1, layer 1 specification*, T1D1.3/86-145R2, Jan. 5 1987.

[43] F. Takawira and D. G. W. Ingram, "Derivation of impulse responses under minimum phase constraints," *Proc. IEE*, vol. 131, pt. F, no. 5, pp. 425–432, Aug. 1984.

[44] E. A. Guillemin, *Theory of Linear Physical Systems*. New York: John Wiley & Sons Inc., 1963.

[45] A. E. Danese, *Advanced Calculus : An Introduction to Applied Mathematics*. Boston, MA: Allyn and Bacon, Inc., 1965.